

Understanding the Biological Context of NS5A–Host Interactions in HCV Infection: A Network-Based Approach

Lokesh P. Tripathi,^{*,¶,†} Hiroto Kambara,^{¶,‡} Yi-An Chen,[†] Yorihiro Nishimura,[‡] Kohji Moriishi,[‡] Toru Okamoto,[‡] Eiji Morita,[‡] Takayuki Abe,[‡] Yoshio Mori,[‡] Yoshiharu Matsuura,[‡] and Kenji Mizuguchi^{*,†,§}

[†]National Institute of Biomedical Innovation, 7-6-8 Saito Asagi, Ibaraki, Osaka, 567-0085, Japan

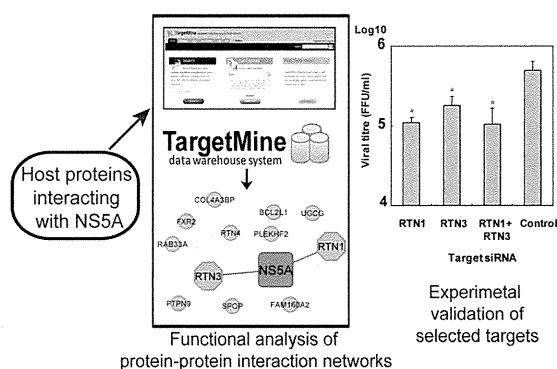
[‡]Department of Molecular Virology, Research Institute for Microbial Diseases, Osaka University, 3-1 Yamada-Oka, Suita, Osaka, 565-0871, Japan

[§]Graduate School of Frontier Biosciences, Osaka University, 1-3 Yamada-Oka, Suita, Osaka, 565-0871, Japan

Supporting Information

ABSTRACT: Hepatitis C virus (HCV) is a major cause of chronic liver disease. HCV NS5A protein plays an important role in HCV infection through its interactions with other HCV proteins and host factors. In an attempt to further our understanding of the biological context of protein interactions between NS5A and host factors in HCV pathogenesis, we generated an extensive physical interaction map between NS5A and cellular factors. By combining a yeast two-hybrid assay with comprehensive literature mining, we built the NS5A interactome composed of 132 human proteins that interact with NS5A. These interactions were integrated into a high-confidence human protein interactome (HPI) with the help of the TargetMine data warehouse system to infer an overall protein interaction map linking NS5A with the components of the host cellular networks. The NS5A–host interactions that were integrated with the HPI were shown to participate in compact and well-connected cellular networks. Functional analysis of the NS5A “infection” network using TargetMine highlighted cellular pathways associated with immune system, cellular signaling, cell adhesion, cellular growth and death among others, which were significantly targeted by NS5A–host interactions. In addition, cellular assays with in vitro HCV cell culture systems identified two ER-localized host proteins RTN1 and RTN3 as novel regulators of HCV propagation. Our analysis builds upon the present understanding of the role of NS5A protein in HCV pathogenesis and provides potential targets for more effective anti-HCV therapeutic intervention.

KEYWORDS: HCV, NS5A, host–pathogen protein–protein interactions, biological network analysis, literature mining, pathway enrichment analysis, siRNA knockdown, target discovery, TargetMine, yeast two-hybrid



INTRODUCTION

Hepatitis C virus (HCV) causes chronic liver disease including liver steatosis, cirrhosis and hepatocellular carcinoma (HCC) and infects nearly 3% of the world population. HCV possesses a single-stranded RNA genome encoding a 3000 amino acid polyprotein, which is processed by host and viral proteases to yield 10 viral proteins, Core, E1, E2, p7, NS2, NS3, NS4A, NS4B, NS5A and NSSB.^{1–5} HCV variants are classified into seven genotypes that display phylogenetic heterogeneity, differences in infectivity and interferon sensitivity.^{6,7} However, despite considerable research, a precise understanding of the molecular mechanisms underlying HCV pathology remains elusive.

HCV NS5A protein (hereafter referred to as NS5A) is a RNA binding phosphoprotein, which consists of three domains; domain I includes a zinc-finger motif necessary for HCV replication and an N-terminal membrane anchor region, and the unstructured domains II and III facilitate protein–protein

interactions. NS5A plays a critical role in regulating viral replication, production of infectious viral particles, interferon resistance and modulation of apoptosis in HCV pathogenesis via interactions with other HCV proteins and host factors.^{8–12} Furthermore, BMS-790052, a small molecule inhibitor of NS5A, is the most potent inhibitor of HCV infection known so far.¹³ Consequently, NS5A has emerged as a unique, attractive and promising target for anti-HCV therapy.^{14–19} In particular, impairing interactions between NS5A and host factors has been shown to impede HCV infection, which may offer novel anti-HCV therapeutic approaches.^{12,20} However, the overall structure and precise functions of NS5A in HCV pathogenesis are poorly understood.

Pathogens such as viruses infect their hosts by interacting with the components of the host cellular networks and

Received: November 30, 2012

Published: May 6, 2013



exploiting the cellular machinery for their survival and propagation. Therefore, elucidating host–pathogen interactions is crucial for a better understanding of pathogenesis.^{21–26} Here, we report the host biological processes likely to be influenced by NSSA by virtue of an inferred protein–protein interaction (PPI) network. We describe our integrated approach that combines an experimental yeast two-hybrid (Y2H) assay using NSSA as bait to screen a library of human cDNAs with comprehensive literature mining. The analysis of the NSSA infection network illustrates the functional pathways likely to be influenced by NSSA–host interactions in HCV pathogenesis, thus providing novel insights into the NSSA function in HCV pathogenesis. Furthermore, RTN1 and RTN3, which are endoplasmic reticulum (ER)-localized proteins involved in regulating ER integrity, will be demonstrated as novel regulators of HCV propagation and thus attractive targets for anti-HCV therapy.

MATERIALS AND METHODS

Yeast Two-Hybrid Protein Assay

Screening for the genes encoding host proteins that interact with NSSA was performed using the Matchmaker two-hybrid system (Clontech, Palo Alto, CA, USA) as per the manufacturers' specifications. Human adult liver libraries were purchased from Clontech and were cloned into the pAct2 vector (Clontech) and expressed as fusion proteins fused to the Gal4-activation domain (Gal4-AD). Since Y2H requires the bait protein to translocate to the nucleus, the cDNA of the region corresponding to the NSSA encoding amino acids 1973–2419 (excluding the NSSA N-terminal membrane anchor region) within the HCV polyprotein from the J1 strain (genotype 1b)²⁷ was amplified by polymerase chain reaction (PCR) and was cloned into the pGBKT7 vector (Clontech)²⁸ and expressed as Gal4-DNA binding domain (Gal4-DB) fusion in the AH109 yeast strain. The human liver libraries were subsequently screened by Y2H using NSSA as bait. A total of 4×10^6 transformants were screened in this manner, and the positive clones (see Supporting Information) were isolated and sequenced to identify the genes coding for the NSSA interacting host factors (Supporting Information, Table S1).

Literature Mining for Pairwise NSSA–Human Interactions

Literature information describing pairwise interactions between NSSA and cellular proteins were extracted from Medline using the PubMed interface and two other information retrieval and extraction tools, EBIMed²⁹ and Protein Corral. These tools employ an automatic text-mining approach, but we supplemented them with a follow-up manual inspection. All abstracts related to “NSSA” and “HCV NSSA” keywords and interaction verbs (including “interact”, “bind”, “attach”, “associate”)³⁰ were gathered and manually examined to retrieve direct pairwise NSSA–human protein interactions (see Supporting Information, Tables S2, S3, S4, S5a).

Construction of Extended Protein–Protein Interaction Networks

Physical and direct binary interactions between all human proteins were retrieved from BioGRID 3.1.93³¹ and iRefindex 9.0³² databases using TargetMine.³³ TargetMine is an integrated data warehouse that combines different types of biological data and employs an objective protocol to prioritize candidate genes for further experimental investigation.³³ The interactions were filtered for redundancy, potential false

positives and isolated components to infer a representative undirected and singly connected high-confidence human protein interactome (HPI) comprising 22 532 nonredundant binary physical interactions between 7277 proteins (see Supporting Information, Figure S2, Table S5b). The inferred HPI was used to identify biologically relevant trends, the significance of which was assessed by using randomized networks (see below). Secondary interactors of the NSSA interacting proteins were retrieved from the HPI and were appended to the NSSA–host interactions to construct a representative NSSA infection network (Supporting Information, Table S5a).

Topological Analysis

Network components were visualized using Cytoscape,^{34,35} while network properties such as *node degree distribution*, *average shortest path* and *betweenness* measures were computed using Cytoscape NetworkAnalyzer plugin³⁶ as described earlier.²⁴ For comparison, degree preserved randomized PPI networks were generated by edge rewiring using the Cytoscape RandomNetworks plugin and were used as control networks to assess the statistical significance of the topological trends observed in the inferred PPI networks (see Supporting Information).

Functional Analysis by Characterization of Enriched Biological Associations

Protein structural domain assignments were retrieved from the Gene3D database,³⁷ Gene ontology associations from the GO consortium,³⁸ and biological pathway data from KEGG³⁹ were used to assign functional annotations to the genes in the NSSA infection network. The enrichment of specific biological associations within the NSSA infection network was estimated by performing the hypergeometric test within TargetMine. The inferred *p*-values were further adjusted for multiple test correction to control the false discovery rate using the Benjamini and Hochberg procedure,^{40,41} and the annotations/pathways were considered significant if the adjusted *p* ≤ 0.005 .

RNAi and Transfection

A mixture of four siRNA targets each to RTN1 and RTN3 (SMARTpool:siGENOME RTN1 siRNA and SMARTpool:siGENOME RTN3 siRNA, respectively) were purchased from Thermo Scientific (Thermo Scientific, Waltham, MA, USA). siGENOME Non-Targeting siRNA Pool #1 (Thermo Scientific) was used as a control siRNA. Thermo Scientific ID numbers of siRNA mixtures of RTN1 and RTN3 and the control were M-014138-00, M-020088-00 and D-001206-13-05, respectively. Each siRNA mixture was introduced into the cell lines by using lipofectamine RNAiMax (Invitrogen, Carlsbad, CA, USA). The replicon cell line, as will be described below, was transfected with each siRNA at a final concentration of 20 nM as per the manufacturer's protocol and then seeded at 2.5×10^4 cells per well of a 24-well plate. The transfected cells were harvested at 72 h post-transfection. The Huh7OK1 cell line, as will be described below, was transfected with each siRNA at a final concentration of 20 nM as per the manufacturer's protocol and then seeded at 2.5×10^4 cells per well of a 24-well plate. The transfected cells were infected with JFH1 at an MOI of 0.05 at 24 h post-transfection. The resulting cells were harvested at the indicated time.

Table 1. List of 132 Human Proteins Interacting with the HCV NSSA Protein

gene ID	symbol	description	refs
47	ACLY	ATP citrate lyase	22
60	ACTB	actin, beta	101
79026	AHNAK	AHNAK nucleoprotein	22
10598	AHSA1	AHA1, activator of heat shock 90 kDa protein ATPase homologue 1 (yeast)	102
207	AKT1	v-akt murine thymoma viral oncogene homologue 1	22
302	ANXA2	annexin A2	103
335	APOA1	apolipoprotein A-I	22
348	APOE	apolipoprotein E	22
116985	ARAP1	ArfGAP with RhoGAP domain, ankyrin repeat and PH domain 1	22
27236	ARFIP1	ADP-ribosylation factor interacting protein 1	22
23204	ARL6IP1	ADP-ribosylation factor-like 6 interacting protein 1	this study
4508	ATP6	ATP synthase F0 subunit 6	this study
8312	AXIN1	axin 1	22
581	BAX	BCL2-associated X protein	22
222389	BEND7	BEN domain containing 7	22
274	BIN1	bridging integrator 1	this study; ^{22,47}
89927	C16orf45	chromosome 16 open reading frame 45	this study
8618	CADPS	Ca ⁺⁺ -dependent secretion activator	22
93664	CADPS2	Ca ⁺⁺ -dependent secretion activator 2	22
79080	CCDC86	coiled-coil domain containing 86	22
983	CDK1	cyclin-dependent kinase 1	22
1021	CDK6	cyclin-dependent kinase 6	22
1060	CENPC1	centromere protein C 1	22
153241	CEP120	centrosomal protein 120 kDa	22
11190	CEP250	centrosomal protein 250 kDa	22
9702	CEP57	centrosomal protein 57 kDa	22
80254	CEP63	centrosomal protein 63 kDa	22
1381	CRABP1	cellular retinoic acid binding protein 1	22
1445	CSK	c-src tyrosine kinase	22
1452	CSNK1A1	casein kinase 1, alpha 1	104
1457	CSNK2A1	casein kinase 2, alpha 1 polypeptide	63,105
1499	CTNNB1	catenin (cadherin-associated protein), beta 1, 88 kDa	84,106
9093	DNAJA3	DnaJ (Hsp40) homologue, subfamily A, member 3	22
2202	EFEMP1	EGF containing fibulin-like extracellular matrix protein 1	22
5610	EIF2AK2	eukaryotic translation initiation factor 2-alpha kinase 2	22
2051	EPHB6	EPH receptor B6	this study
54942	FAM206A	family with sequence similarity 206, member A	22
25827	FBXL2	F-box and leucine-rich repeat protein 2	22
2274	FHL2	four and a half LIM domains 2	22
23770	FKBP8	FK506 binding protein 8, 38 kDa	this study; ^{43,45}
2316	FLNA	filamin A, alpha	12
2495	FTH1	ferritin, heavy polypeptide 1	22
8880	FUBP1	far upstream element (FUSE) binding protein 1	107
2534	FYN	FYN oncogene related to SRC, FGR, YES	22
11345	GABARAPL2	GABA(A) receptor-associated protein-like 2	this study
54826	GIN1	gypsy retrotransposon integrase 1	22
2801	GOLGA2	golgin A2	22
2874	GPS2	G protein pathway suppressor 2	22
2885	GRB2	growth factor receptor-bound protein 2	22
2931	GSK3A	glycogen synthase kinase 3 alpha	22
2932	GSK3B	glycogen synthase kinase 3 beta	22
3055	HCK	hemopoietic cell kinase	22
3320	HSP90AA1	heat shock protein 90 kDa alpha (cytosolic), class A member 1	22
3303	HSPA1A	heat shock 70 kDa protein 1A	108
3315	HSPB1	heat shock 27 kDa protein 1	109
3537	IGLC1	immunoglobulin lambda constant 1 (Mcg marker)	22
79711	IPO4	importin 4	22
3843	IPO5	importin 5	22
3683	ITGAL	integrin, alpha L (antigen CD11A (p180), lymphocyte function-associated antigen 1; alpha polypeptide)	22
6453	ITSN1	intersectin 1	this study
3716	JAK1	Janus kinase 1	22

Table 1. continued

gene ID	symbol	description	refs
3932	LCK	lymphocyte-specific protein tyrosine kinase	22
55679	LIMS2	LIM and senescent cell antigen-like domains 2	22
4067	LYN	v-yes-1 Yamaguchi sarcoma viral related oncogene homologue	22
9448	MAP4K4	mitogen-activated protein kinase kinase kinase kinase 4	this study
6300	MAPK12	mitogen-activated protein kinase 12	22
4155	MBP	myelin basic protein	22
4256	MGP	matrix Gla protein	110
55233	MOB1A	MOB kinase activator 1A	22
4673	NAP1L1	nucleosome assembly protein 1-like 1	22
4674	NAP1L2	nucleosome assembly protein 1-like 2	22
10397	NDRG1	N-myc downstream regulated 1	22
4778	NFE2	nuclear factor (erythroid-derived 2), 45 kDa	22
11188	NISCH	nischarin	this study
4924	NUCB1	nucleobindin 1	22
4938	OAS1	2'-5'-oligoadenylate synthetase 1, 40/46 kDa	22
5007	OSBP	oxysterol binding protein	111
64098	PARVG	parvin, gamma	22
5170	PDPK1	3-phosphoinositide dependent protein kinase-1	22
5297	PI4KA	phosphatidylinositol 4-kinase, catalytic, alpha	22
5291	PIK3CB	phosphoinositide-3-kinase, catalytic, beta polypeptide	22
5295	PIK3R1	phosphoinositide-3-kinase, regulatory subunit 1 (alpha)	55,84,106
5300	PIN1	peptidylprolyl cis/trans isomerase, NIMA-interacting 1	112
5307	PITX1	paired-like homeodomain 1	22
5347	PLK1	polo-like kinase 1	113
10654	PMVK	phosphomevalonate kinase	22
5478	PPIA	peptidylprolyl isomerase A (cyclophilin A)	114,115
10848	PPP1R13L	protein phosphatase 1, regulatory subunit 13 like	22
5515	PPP2CA	protein phosphatase 2, catalytic subunit, alpha isozyme	116
5518	PPP2R1A	protein phosphatase 2, regulatory subunit A, alpha	116
5698	PSMB9	proteasome (prosome, macropain) subunit, beta type, 9 (large multifunctional peptidase 2)	22
5757	PTMA	prothymosin, alpha	22
5894	RAF1	v-raf-1 murine leukemia viral oncogene homologue 1	22
6142	RPL18A	ribosomal protein L18a	22
6167	RPL37	ribosomal protein L37	this study
6238	RRBP1	ribosome binding protein 1 homologue 180 kDa (dog)	22
91543	RSAD2	radical S-adenosyl methionine domain containing 2	117
6252	RTN1	reticulon 1	this study
10313	RTN3	reticulon 3	this study
6424	SFRP4	secreted frizzled-related protein 4	22
81858	SHARPIN	SHANK-associated RH domain interactor	22
64754	SMYD3	SET and MYND domain containing 3	22
8470	SORBS2	sorbin and SH3 domain containing 2	22
10174	SORBS3	sorbin and SH3 domain containing 3	22
6714	SRC	v-src sarcoma (Schmidt-Ruppin A-2) viral oncogene homologue (avian)	22
10847	SRCAP	Snf2-related CREBBP activator protein	22
6741	SSB	Sjogren syndrome antigen B (autoantigen La)	22
284297	SSC5D	scavenger receptor cysteine rich domain containing (5 domains)	110
6772	STAT1	signal transducer and activator of transcription 1	118
25777	SUN2	Sad1 and UNC84 domain containing 2	this study
6850	SYK	spleen tyrosine kinase	119
4070	TACSTD2	tumor-associated calcium signal transducer 2	22
6880	TAF9	TAF9 RNA polymerase II, TATA box binding protein (TBP)-associated factor, 32 kDa	22
6908	TBP	TATA box binding protein	22
7046	TGFBR1	transforming growth factor, beta receptor 1	22
7057	THBS1	thrombospondin 1	22
374395	TMEM179B	transmembrane protein 179B	22
7110	TMF1	TATA element modulatory factor 1	22
7157	TP53	tumor protein p53	22
7159	TP53BP2	tumor protein p53 binding protein, 2	22
7186	TRAF2	TNF receptor-associated factor 2	22
11078	TRIOBP	TRIO and F-actin binding protein	22

Table 1. continued

gene ID	symbol	description	refs
51061	TXNDC11	thioredoxin domain containing 11	22
53347	UBASH3A	ubiquitin associated and SH3 domain containing A	22
10869	USP19	ubiquitin specific peptidase 19	22
9218	VAPA	VAMP (vesicle-associated membrane protein)-associated protein A, 33 kDa	22
9217	VAPB	VAMP (vesicle-associated membrane protein)-associated protein B and C	this study; 22,28,46
10493	VAT1	vesicle amine transport protein 1 homologue (<i>T. californica</i>)	this study
55737	VPS35	vacuolar protein sorting 35 homologue (<i>S. cerevisiae</i>)	22
6293	VPS52	vacuolar protein sorting 52 homologue (<i>S. cerevisiae</i>)	22
140612	ZFP28	zinc finger protein 28 homologue (mouse)	this study
9726	ZNF646	zinc finger protein 646	22

Quantitative Reverse-Transcription PCR (qRT-PCR)

Total RNA was prepared from the cell and culture supernatant using the RNeasy mini kit (QIAGEN, Hilden, Germany) and QIAamp Viral RNA Mini Kit (QIAGEN), respectively. First-strand cDNA was synthesized using high capacity cDNA reverse transcription kit (Applied biosystems, Carlsbad, CA, USA) with random primers. Each cDNA was estimated by Platinum SYBR Green qPCR Super Mix UDG (Invitrogen) as per the manufacturer's protocol. Fluorescent signals of SYBR Green were analyzed with ABI PRISM 7000 (Applied Biosystems). The HCV internal ribosomal entry site (IRES) region and human glyceraldehyde-3-phosphate dehydrogenase (GAPDH) gene were amplified with the primer pairs 5'-GAGTGTCTCGTGCAGCCTCCA-3' and 5'-CACTCGCAAGCACCTATCA-3', and 5'-GAAGGTCGGAGTCAACGGATT-3' and 5'-GATGACAAGCTTCCCGTTCTC-3', respectively.⁴² The quantities of the HCV genome and the other host mRNAs were normalized with that of GAPDH mRNA. RTN1 and RTN3 genes were amplified using the primer pairs purchased from QIAGEN.

Cell Lines and Virus Infection

Cells from the Huh7OK1 cell line are highly permissive to HCV JFH1 strain (genotype 2a) infection compared to Huh 7.5.1 and exhibit the highest propagation efficiency for JFH1.⁴³ These cells were maintained at 37 °C in a humidified atmosphere and 5% CO₂, in the Dulbecco's modified Eagle's medium (DMEM) (Sigma, St. Louis, MO, USA) supplemented with nonessential amino acids (NEAA) and 10% fetal calf serum (FCS). The viral RNA of JFH1 was introduced into Huh7OK1 as described by Wakita et al.⁴⁴ The viral RNA of JFH1 derived from the plasmid pJFH1 was prepared as described by Wakita et al.⁴⁴

Statistical Analysis

Experiments for RNAi transfection and qRT-PCR were performed two times. The estimated values were represented as the mean \pm standard deviation ($n = 2$). The significance of differences in the means was determined by the Student's *t*-test.

RESULTS AND DISCUSSION

Identifying Host Proteins That Interact with HCV NS5A Protein

We employed an integrated approach that combined an experimental Y2H assay and comprehensive literature mining to identify human host proteins interacting with NS5A.

First, we performed an Y2H screening to characterize the interactions between NS5A and host proteins. The analysis of positive colonies revealed 17 host factors as interacting partners

of NS5A (Tables 1, S1, Supporting Information), 14 of which are novel. The other three interactions have been characterized previously; vesicle-associated membrane protein (VAMP)-associated protein B (VAPB), a membrane trafficking factor, and FK506-binding protein 8 (FKBP8), an immunoregulation protein, independently regulate HCV replication via interactions with NS5A;^{28,43,45,46} Bridging integrator 1 (BIN1), a tumor suppressor protein, interacts with NS5A and significantly contributes to HCC.⁴⁷ Among the newly discovered interactors, MAP4K4 is overexpressed in HCC, and knock-down of MAP4K4 expression inhibits HCC progression;⁴⁸ RTN1 and VAT1 were previously observed to be elevated in HCV infected cells,⁴⁹ and ARL6IP1, EPHB6, GABARAPL2, ITSN1 and NISCH were differentially expressed in HCV infection in vitro.⁵⁰ Furthermore, five (ARL6IP1, FKBP8, RTN1, RTN3, VAPB) of the 17 interactors (29.4%) localize to the endoplasmic reticulum (ER; GO:0005783; $p = 0.0028$), which is consistent with the role of NS5A as a crucial constituent of the HCV replication complex associated with the ER.⁵¹ These results suggest that the PPIs detected by our Y2H assay may closely reflect NS5A interactions in vivo.

We next scanned the biomedical literature to expand the repertoire of NS5A–host interactions. Because of an ever increasing volume of biomedical literature describing the pathogenesis of infectious diseases, the identification of specific host–pathogen interactions and their roles in pathogenicity is a nontrivial task, and therefore, recent years have witnessed a rapid development of computational tools for biomedical literature mining. We performed extensive literature mining using computational tools that facilitate the retrieval and extraction of relevant information from the biomedical literature (Pubmed, EBIMed, Protein Coral) and followed it up with a careful manual inspection to identify additional host factors, which directly interact with NS5A and which were not present in the Y2H data set. One hundred and fifteen pairwise interactions between NS5A and human proteins (consisting of 93 catalogued by a high throughput study of binary HCV–host interactions²² and 22 from assorted reports; see Supporting Information, Table S2) were extracted from the literature in this manner and were added to the existing interactors. The resulting NS5A–human interactome thus comprised 132 human host proteins directly interacting with NS5A (Table 1), all of which are expressed in the liver (see Supporting Information, Table S3).

Network Topological Analysis of the NS5A–host Interactions: NS5A Preferentially Targets Hubs and Bottlenecks in the Host Protein Interactome

To further understand the biological significance of the NS5A–host interactions, we retrieved PPIs for the nodes targeted by

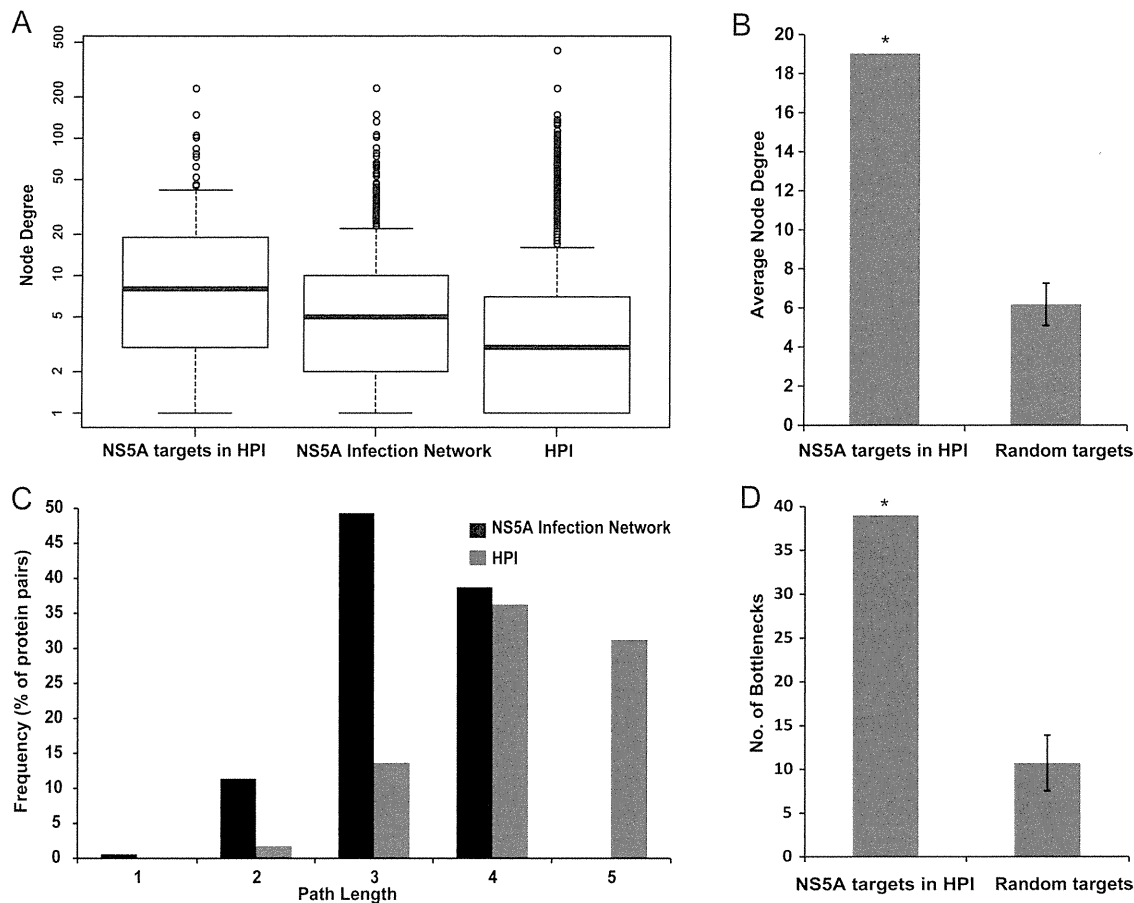


Figure 1. Topological analysis of the NSSA infection network. (A) The node degree distributions of the NSSA interactors in the HPI, NSSA infection network, and HPI are represented as box plots. The average degree of the NSSA interactors in HPI (19.02) was higher than those of the NSSA infection network (8.24) and HPI (5.96). Median node degrees (indicated by thick horizontal lines) of the NSSA interactors in HPI, NSSA infection network, and HPI are 8, 5, and 3, respectively. (B) The average degree of the nodes targeted by NSSA in HPI was much higher than mean average degree of 1000 sets of the randomly selected 108 nodes in HPI. (C) The shortest path length distributions of the NSSA infection network and HPI. The path length is represented on the x-axis while the y-axis describes the frequency, i.e., the percentage of node (protein) pairs within the PPI network with a given shortest path length. For simplicity, only the node frequencies for path lengths 1–5 in the HPI are displayed. (D) The number of bottlenecks among the nodes targeted by NSSA in HPI was much higher than mean of the number of bottlenecks among 1000 sets of the randomly selected 108 nodes in HPI. *: $p < 0.001$.

NSSA in the HPI and incorporated them with the initial interactions to infer an extended NSSA infection network. PPIs for 108 of 132 NSSA interactors were retrieved in this manner; 24 of 132 NSSA interactors had no PPIs in the HPI (Supporting Information, Tables S4, S5a, S5b). For the NSSA infection network and the HPI, we computed the node degree distribution and the characteristic/average path length measures to capture the topologies of the two networks. The degree of a protein, which corresponds to the number of its interacting partners, may often reflect its biological relevance since a better connected protein is likely to have a higher ability to influence biological networks via PPIs. Average path lengths provide an approximate measure of the relative ease and speed of dissemination of information between the proteins in a network.

The NSSA infection network consisted of 1442 entities (nearly all of which are expressed in the liver; see Supporting Information) with 6263 interactions between them (Supporting Information, Tables S4, S5a). The average degree (defined as the number of interactions for a given protein) of the NSSA infection network (8.24) was notably higher than the degree inferred for the HPI (5.96) (Figure 1A). Furthermore, the

average degree of the nodes targeted by NSSA in the HPI (19.02) was even higher; this number is significantly greater than the average degree obtained from a sample of randomly selected nodes (6.17 ± 1.08 with $p < 0.001$; Figure 1B; see Supporting Information). Also the degrees inferred for the majority of the NSSA interactors in the HPI (65 of 108; 60.18%) were higher than the mean degree of the HPI (5.96) (Figure 1A). Our observations therefore suggest that NSSA preferentially targets several highly connected cellular proteins (hubs) with an ability to influence a large number of host factors in HCV infection. The average (shortest) path length of the NSSA infection network (3.26) was significantly shorter than the HPI (4.54), and also the distribution of shortest path lengths was shifted toward the left (Figure 1C), thereby suggesting that the NSSA influenced cellular network is more compact and inclined toward faster communication between the constituents relative to the host cellular network.

Next, we examined the betweenness measures of the NSSA interactors in the HPI to assess their significance in the HPI and the NSSA infection network. The betweenness of a node, determined by the number of shortest paths passing through it, reflects the importance of that node in the network; the nodes

with the highest betweenness prominently regulate the flow of signaling information and are therefore “bottlenecks”, representing central points for communication in an interaction network.⁵² Previously, proteins with high betweenness have been implicated in crucial roles in HCV infection and pathogenesis.^{53,54} To investigate if NSSA preferentially targets bottlenecks (defined as the top 10% of the nodes in the HPI ranked by betweenness), we estimated the fraction of NSSA interactors that were bottlenecks in the HPI. A significant proportion (39 of 108; 36.1%) of the NSSA interactors were identified as bottlenecks in the HPI (Supporting Information, Table S6); this number is significantly higher than the number of bottlenecks among randomly selected nodes (10.72 ± 3.17 with $p < 0.001$; Figure 1D; see Supporting Information). These include growth factor receptor-binding protein 2 (GRB2), which plays an important role in the subversion of host signaling pathways by NSSA,⁵⁵ tumor protein 53 (TP53), a key mediator of the oncogenic effect of NSSA in HCV-induced HCC;⁵⁶ and tyrosine kinase SRC, which regulates the formation of NSSA-containing HCV replication complex.⁵⁷ Among the NSSA interacting proteins identified by our Y2H screening, ITSN1, an endocytic traffic associated protein, and GABARAPL2, an autophagy associated protein, were identified as network bottlenecks.

Our observations therefore suggest that NSSA preferentially interacts with highly central proteins in the host protein interactome; these interactions may help the virus to regulate efficiently the flow of the infection-related information in the host cellular network and manipulate the host metabolic machinery for its own survival and pathogenesis. Our observations are consistent with studies that suggested that viral pathogens tend to interact with well-connected host proteins that are central to the host cellular networks, thus enabling them to appropriate essential cellular functions.^{21,22,26,58,59}

Functional Analysis of NSSA Interaction Network

Next, we investigated the NSSA infection network for the enrichment of specific biological associations (KEGG pathways, CATH structural domains; GO terms and Reactome Pathways; Supporting Information, Tables S7a, S7b, S7c and S7d). Notably, a significant proportion of the proteins in the NSSA infection network were mapped to the CATH Phosphorylase Kinase; domain 1, domain (CATH:3.30.200.20; 138 out of 1442, $p = 2.61 \times 10^{-45}$) including 23 of the 132 NSSA interacting host proteins ($p = 3.38 \times 10^{-14}$) (13 of which are bottlenecks in the HPI), based on the Gene3D protein domain assignments (Supporting Information, Table S7b). These include two novel interactions between EPHB6 (a kinase deficient receptor) and MAP4K4 and NSSA, identified by our Y2H assay (Table 1). The significant representation of cellular kinases in the NSSA infection network is consistent with the key roles played by reversible phosphorylation of NSSA in modulating various NSSA functions in HCV pathogenesis. Impairing NSSA hyperphosphorylation has been shown to inhibit HCV replication, and thus, the cellular kinases that regulate NSSA phosphorylation are important targets for anti-HCV therapy.^{9,60–63}

The analysis of NSSA infection network revealed an enrichment of 79 KEGG pathways (Supporting Information, Table S7a). Furthermore, 31 of the 39 NSSA interacting bottlenecks (hereafter referred to as bottlenecks) were mapped to 75 of the 79 enriched KEGG pathways (Supporting

Information, Table S5). Among the 75 bottleneck-associated enriched KEGG pathways, the highest numbers were associated with various cancers and infectious diseases (31 enriched KEGG pathways; 27 bottlenecks), followed by immune system, signal transduction and endocrine system (23 enriched KEGG pathways; 27 bottlenecks), cell growth and death (4 enriched KEGG pathways; 9 bottlenecks), nervous system (4 enriched KEGG pathways; 8 bottlenecks) and cellular communication (3 enriched KEGG pathways; 14 bottlenecks) among others (Tables 2, S8a, Supporting Information). Below we describe our observations on the most prominent enriched biological themes of interest that were associated with the NSSA infection network, with a specific focus on the bottlenecks.

Cancers and Infectious Diseases

The analysis of the NSSA interaction network revealed that NSSA specifically targets host factors that participate in various complex human diseases. Thirty-four NSSA interactors including 24 bottlenecks were mapped to one or more of the 17 enriched KEGG pathways associated with different infectious diseases (Supporting Information, Tables S7a, S8a). Among the most prominent associations, 12 bottlenecks were mapped to “Epstein–Barr virus infection” ($p = 1.36 \times 10^{-27}$); 10 to “Hepatitis C” ($p = 3.47 \times 10^{-24}$); 10 to “HTLV-I infection” ($p = 1.39 \times 10^{-20}$); 9 to “Hepatitis B” ($p = 3.33 \times 10^{-26}$); 8 to “Measles” ($p = 5.69 \times 10^{-17}$); 7 bottlenecks were mapped to “Influenza A” ($p = 5.01 \times 10^{-12}$); 7 to “Herpes simplex infection” ($p = 1.47 \times 10^{-13}$) and 6 to “Tuberculosis” ($p = 3.02 \times 10^{-6}$) (Supporting Information, Tables S7a, S8a). These associations include infectious diseases induced by various bacterial and viral pathogens thereby suggesting that HCV and other pathogens may systematically target specific host factors, the perturbation of which may contribute to the onset of various human diseases.

Also, 19 bottlenecks were mapped to one or more of the 16 enriched KEGG pathways associated with various cancers. Among the most prominent associations, 10 bottlenecks were mapped to “Viral carcinogenesis” ($p = 1.3 \times 10^{-30}$); 8 each were mapped to “Prostate cancer” ($p = 4.27 \times 10^{-25}$), “Endometrial cancer” ($p = 5.52 \times 10^{-21}$) and “Colorectal cancer” ($p = 4.22 \times 10^{-18}$); 7 to “Pancreatic cancer” ($p = 1.94 \times 10^{-18}$); 6 to “Chronic myeloid leukemia” ($p = 1.61 \times 10^{-30}$) and 5 each to “Non-small cell lung cancer” ($p = 8.66 \times 10^{-15}$) and “Glioma” ($p = 2.38 \times 10^{-14}$) (Supporting Information, Tables S7a, S8a). The significant association of HCV with host factors central to various cancer pathways (including tumor suppressors such as TP53) is consistent with previous observations that viral pathogens significantly targeted host proteins associated with cancer pathways,^{59,64,65} which likely plays major roles in tumorigenesis.

Immune System and Signal Transduction

HCV infection induces various active and passive host immune responses including the recognition of viral RNA by host cell receptors. These events lead to the production of Type I interferons (IFN- α/β) and inflammatory cytokines in the infected hepatocytes, initiating the antiviral response. HCV persistence in the host is determined by the virus’s ability to impair host immune responses.^{66–69}

The analysis of the NSSA interaction network revealed that 21 of the 132 NSSA interacting proteins, including 16 bottlenecks and their interacting partners, were mapped to one or more enriched KEGG pathways associated with the immune system (Supporting Information, Tables S7a, S8a).

Table 2. KEGG Pathway Functional Categories (Subclasses) Sorted by the Number of Enriched Pathways (≥ 3) Associated with One or More NSSA Interacting Bottlenecks

category	no. of enriched pathways	no. of bottlenecks	associated bottlenecks	KEGG pathways in the given category associated with most number of bottlenecks
infectious diseases	16	24	ACTB, AKT1, CDK1, CSNK2A1, CTNNB1, FLNA, FYN, GSP2, GRB2, GSK3B, HSPB1, JAK1, LCK, LYN, PIK3R1, PPP2CA, RAF1, SRC, STAT1, SYK, TBP, TGFBR1, TP53, TRAF2	"Epstein-Barr virus infection"; "HTLV-1 infection"; "Hepatitis C"; "Hepatitis B"; "Measles"; "Influenza A"; "Herpes simplex infection"; "Tuberculosis"; "Toxoplasmosis"; "Chagas disease (American trypanosomiasis)"; "Bacterial invasion of epithelial cells"
cancers	16	19	AKT1, AXIN1, CDK1, CTNNB1, GRB2, GSK3B, HSP90AA1, JAK1, LYN, RAF1, SRC, STAT1, SYK, TBP, TGFBR1, THBS1, TP53, TRAF2	"Pathways in cancer"; "Viral carcinogenesis"; "Prostate cancer"; "Endometrial cancer"; "Colorectal cancer"; "Pancreatic cancer"; "Chronic myeloid leukemia"; "Non-small cell lung cancer"; "Glioma"; "Small cell lung cancer"; "Renal cell carcinoma"; "Melanoma"; "Acute myeloid leukemia"
immune system	10	16	ACTB, AKT1, CTNNB1, FYN, GRB2, GSK3B, HSP90AA1, LCK, LYN, PIK3R1, PIN1, RAF1, SRC, STAT1, SYK, TRAF	"Chemokine signaling pathway"; "T cell receptor signaling pathway"; "Fc epsilon RI signaling pathway"; "B cell receptor signaling pathway"; "Natural killer cell mediated cytotoxicity"; "Fc gamma R-mediated phagocytosis"
signal transduction	9	22	AKT1, AXIN1, CSKN1A1, CTNNB1, FLN, GRB2, GSK3B, HSP90AA1, HSPB1, JAK1, LCK, LYN, PIK3R1, PPP2CA, RAF1, SRC, STAT1, SYK, TGFBR1, THBS1, TP53, TRAF2	"PI3K-Akt signaling pathway"; "MAPK signaling pathway"; "Wnt signaling pathway"; "ErbB signaling pathway"; "VEGF signaling pathway"; "NF-kappa B signaling pathway"; "Jak-STAT signaling pathway"
nervous system	5	8	AKT1, GRB2, GSK3B, LYN, PIK3R1, PPP2CA, RAF1, TP53	"Neurotrophin signaling pathway"; "Long-term depression"; "Dopaminergic synapse"; "Long-term potentiation"
endocrine system	4	10	AKT1, CDK1, GRB2, GSK3B, HSP90AA1, PIK3R1, PLK1, RAF1, SRC, TRAF2	"Progesterone-mediated oocyte maturation"; "Insulin signaling pathway"; "GnRH signaling pathway"; "Adipocytokine signaling pathway"
cell growth and death	4	9	AKT1, CDK1, GSK3B, PIK3R1, PLK1, PPP2CA, THBS1, TP53, TRAF2	"Cell cycle"; "Apoptosis"; "p53 signaling pathway"; "Oocyte meiosis"
cell communication	3	14	ACTB, AKT1, CSNK2A1, CTNNB1, FLNA, FYN, GRB2, GSK3B, PIK3R1, PPP2CA, RAF1, SRC, TGFBR1, THBS1	"Focal adhesion"; "Tight junction"; "Adherens junction"
development	3	12	AKT1, FHL2, FYN, GRB2, GSK3B, JAK1, LCK, PIK3R1, STAT1, SYK, TGFBR1, THBS1	"Osteoclast differentiation"; "Axon guidance"; "Dorso-ventral axis formation"

Eight bottlenecks were mapped to the enriched KEGG pathway "Chemokine signaling pathway" ($p = 2.27 \times 10^{-10}$), which is consistent with the modulation of host interferon signaling by NSSA in HCV infection.⁷⁰ In addition, 7 bottlenecks each were mapped to "T cell receptor signaling pathway" ($p = 4.6 \times 10^{-24}$), "Fc epsilon RI signaling pathway" ($p = 2.86 \times 10^{-14}$) and "B cell receptor signaling pathway" ($p = 1.8 \times 10^{-14}$) and 6 bottlenecks were mapped to "Natural killer cell mediated cytotoxicity" ($p = 1.92 \times 10^{-12}$). Three bottlenecks (AKT1, PIK3R1 and STAT1) were also mapped to the enriched KEGG pathway "Toll-like receptor signaling pathway" ($p = 3.23 \times 10^{-7}$; Supporting Information, Tables S7a, S8a). Toll-like receptor 3 mediated chemokine and cytokine signaling plays an important role in the host immune response in HCV infection.⁷¹ Therefore, NSSA interaction with bottlenecks, which function in various aspects of the host immune response, may significantly contribute to the perturbation of the host immune system in HCV pathogenesis.

Additionally, 32 of 132 NSSA interacting proteins examined in the present study, including 24 bottlenecks, were mapped to various pathways associated with the signal transduction and the endocrine system (Supporting Information, Tables S7a, S8a), many of which are implicated in HCV infection and HCC progression and are targets for molecular therapy in HCC.^{22,72-74}

Eleven bottlenecks were mapped to the enriched KEGG pathway "PI3K-Akt signaling pathway" ($p = 2.2 \times 10^{-24}$; Supporting Information, Tables S7a, S8a), which is consistent with a previous study that NSSA stimulates the activation of PI3K-Akt pathway, which contributes to HCC in HCV infection.⁷⁵ Eight bottlenecks were mapped to the enriched KEGG pathway "MAPK signaling pathway" ($p = 2.4 \times 10^{-19}$; Supporting Information, Tables S7a, S8a). Elements of the MAPK signaling cascades are directly involved in the progression of HCV infection, particularly in association with HCV Core and E2 proteins,^{22,24,76,77} thereby suggesting that NSSA interactions with the key facilitators of MAPK signaling in the host interactome may play an important role in regulating the reversible phosphorylation of NSSA and may contribute to the progression of HCV pathogenesis.

Bottlenecks AKT1, GRB2, GSK3B, PIK3R1 and RAF1 and many of their interactors were mapped to the enriched KEGG pathway "Insulin signaling pathway" ($p = 2.42 \times 10^{-13}$; Supporting Information, Tables S7a, S8a); these proteins are highlighted in Figure 2. Insulin signaling plays an important role in regulating glucose and lipid metabolism, and the disruption of this process may contribute to insulin resistance (IR). IR is linked with steatosis, fibrosis progression and poor interferon- α response in HCV infection.⁷⁸⁻⁸⁰ Suppression of AKT1 and GSK3B activity in HCV infection disrupts glucose metabolism and contributes to IR.^{81,82} Furthermore, PIK3R1 and NSSA interactor PIK3CB (Figure 2) are subunits of phosphatidylinositol 3-kinase (PI3K), which controls insulin secretion,⁸³ PI3K also facilitates the activation of the proto-oncogene beta-catenin (CTNNB1) by NSSA, which contributes to the development of HCC in HCV pathogenesis.⁸⁴ Previously, HCV Core protein has been directly implicated in the induction of IR in HCV infection,⁸⁵ while there is little evidence suggesting definitive links between NSSA and IR. Our observations, however, suggest that NSSA directly interacts with key regulators of insulin metabolism and may, therefore, play a major role in modulating HCV-induced IR and eventually HCC.

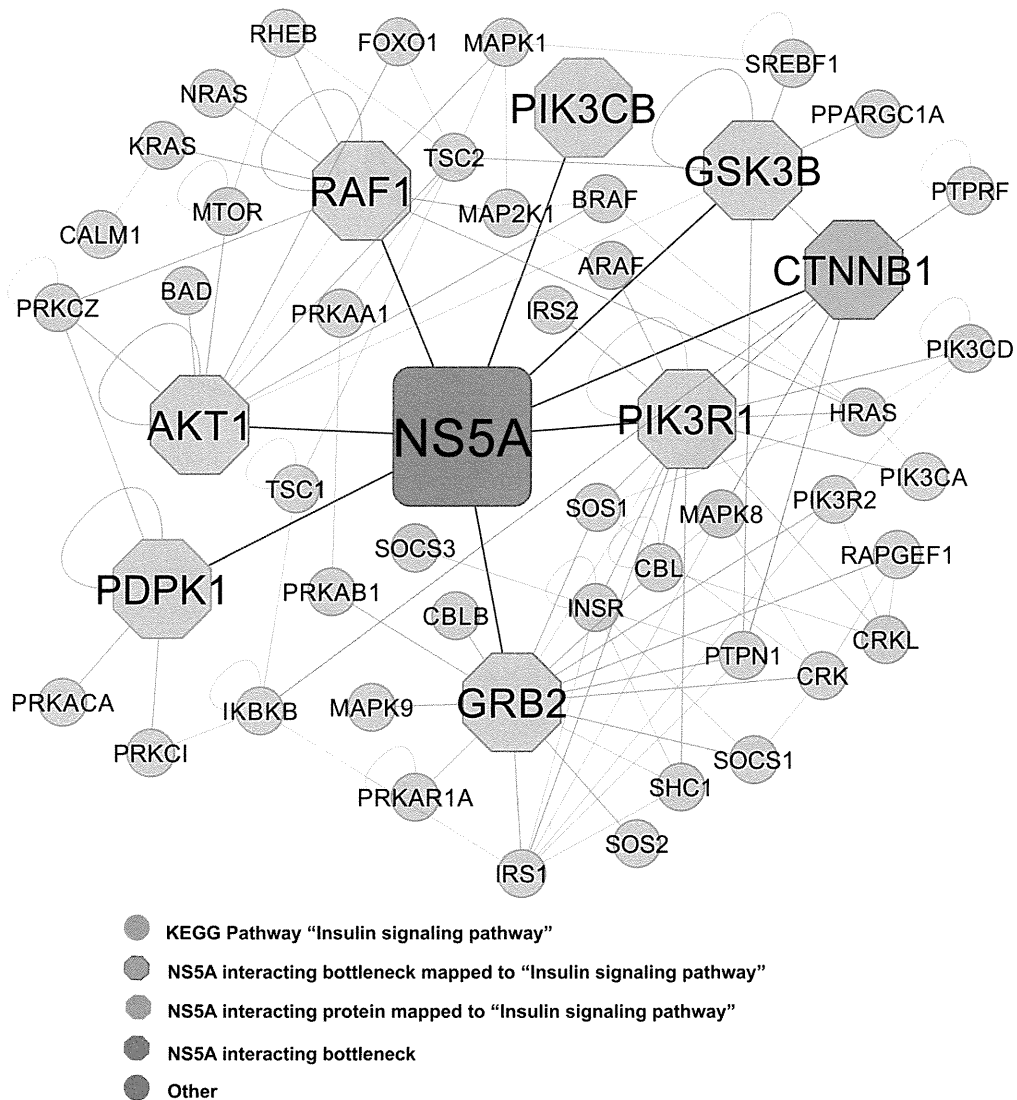


Figure 2. NS5A interacting bottlenecks and their interacting partners associated with the enriched KEGG pathway hsa04910: "Insulin signaling pathway".

Cell Adhesion and Communication

The perturbation of adherens and tight junction associated proteins has been implicated in HCV entry, cell–cell transmission and hepatoma migration in HCV infection.^{86–88} In the NS5A infection network, eight bottlenecks (ACTB, AKT1, CSNK2A1, CTNNB1, FYN, PPP2CA, SRC and TGFBR1) were mapped to either or both of the enriched KEGG pathways "Adherens Junction" ($p = 1.03 \times 10^{-15}$) and "Tight junction" ($p = 1.19 \times 10^{-5}$), which are associated with cell adhesion junctions and cellular communication (Supporting Information, Tables S7a, S8a). CSNK2A1 is the catalytic (alpha) subunit of Casein Kinase II (CK2), which phosphorylates NS5A and regulates the production of infectious viral particles.⁶³ CTNNB1, a key component of cell-adhesion complexes, is positively regulated by CK2.⁸⁹ Furthermore, the activation of CTNNB1 by NS5A significantly contributes to HCC.⁸⁴ Taken together, our observations suggest that NS5A interactions with bottlenecks, which regulate cell–cell adhesion (CSNK2A1, CTNNB1) and cytoskeletal organization (ACTB), may significantly contribute to the progression of HCV life cycle and tumorigenesis in HCV pathogenesis.

Eleven bottlenecks were mapped to the enriched KEGG pathway "Focal Adhesion" ($p = 1.02 \times 10^{-17}$; Supporting Information, Tables S7a, S8a), thereby reiterating that focal adhesion is a major target of NS5A.²² Focal adhesion regulates cell migration and adhesion, and some of its components were directly implicated in the regulation of HCV replication and propagation in our earlier study.²⁴ Our observations thus suggest that NS5A interactions with key components of the focal adhesion machinery may play important roles in the HCV lifecycle. For instance, NS5A interacts with bottleneck THBS1 (Thrombospondin-1), a glycoprotein, which was mapped to the KEGG "Focal Adhesion" pathway. THBS1 plays a key role in NS5A-mediated activation of the cytokine TGF- β 1, which facilitates HCV replication and progressive liver fibrosis in HCV infection.⁹⁰ Our observations suggest that direct NS5A interactions with the bottlenecks THBS1 and TGFBR1 (TGF- β receptor 1; KEGG Pathway "Adherens Junction"), a key facilitator of TGF- β downstream signaling, may be crucial in facilitating HCV replication and tumorigenesis in HCV pathogenesis.

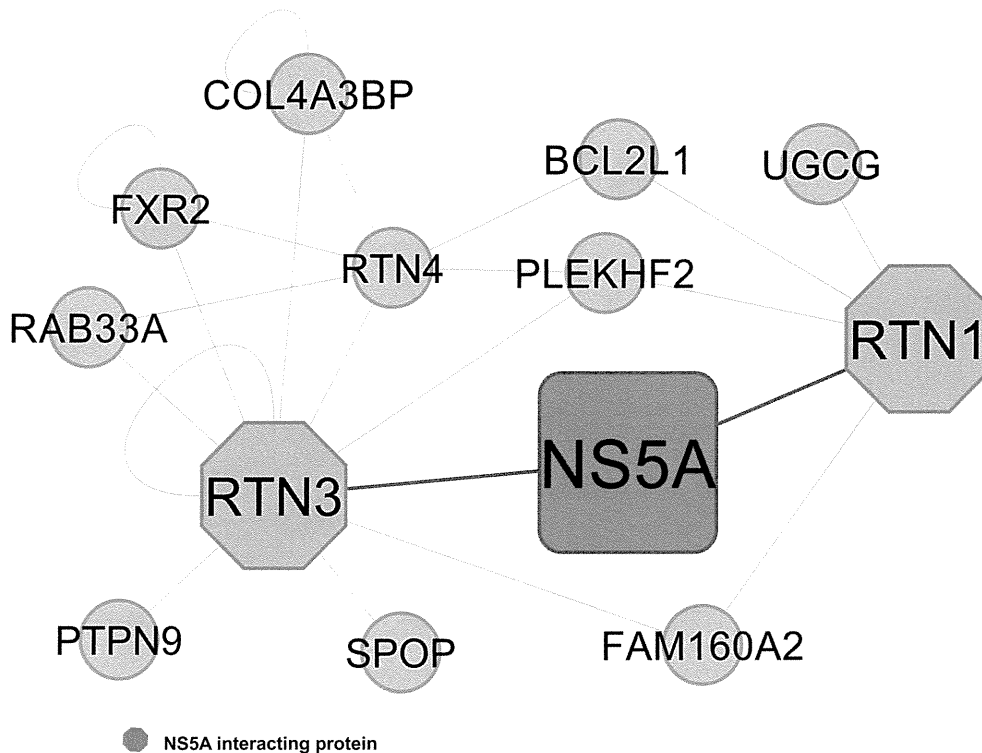


Figure 3. ER-localized host factors RTN1 and RTN3 were found to interact (blue edges) with NS5A in a Y2H screening of human liver cDNA library using NS5A as bait.

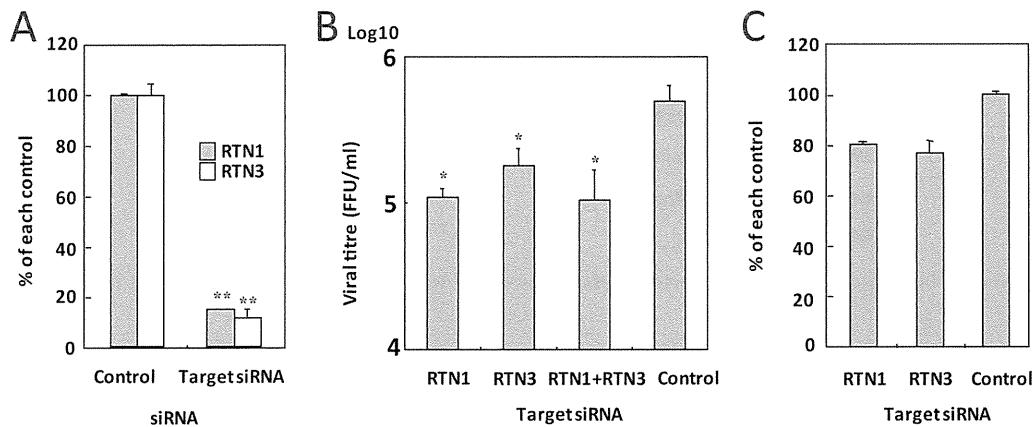


Figure 4. Effects of knockdown of RTN1 and RTN3 on HCV propagation and replication. Host factors RTN1 and RTN3 were suppressed by RNAi (A) in Huh7OK1 cells infected with HCV JFH1 strain (genotype 2a). The amounts of viral titer (B) and intracellular viral RNA (C) were estimated. Each value was represented as percentage of the cells transfected with the control siRNA. FFU: Focus-forming units; *, $p < 0.05$, **, $p < 0.01$.

Cellular Transport

Cellular factors associated with endocytic trafficking are key facilitators of the HCV life cycle, particularly HCV entry into the hepatic cells.^{91–93} Endocytosis of the extracellular growth factor receptor (EGFR) in association with the cell surface glycoprotein CD81 plays a crucial role in HCV internalization and entry and is, therefore, an attractive target of anti-HCV strategies.⁹⁴ In the NS5A infection network, NS5A interactors ARAP1 and HSPA1A together with two bottlenecks (SRC, TGFBR1) were mapped to the enriched KEGG pathway “Endocytosis” ($p = 2.97 \times 10^{-8}$; Supporting Information, Tables S7a, S8a). ARAP1, a Golgi associated protein, negatively regulates EGFR trafficking, and decreased ARAP1 expression contributes to enhanced EGFR endocytosis.⁹⁵ Therefore, NS5A

interaction with ARAP1 may facilitate EGFR internalization and thus viral entry in HCV infection.

NS5A Interacting Host Proteins RTN1 and RTN3 Function in HCV Propagation but Not Replication

Traditionally, viral and host proteins associated with the HCV lifecycle (internalization, replication, assembly and release) have been preferred targets in the anti-HCV studies. During infection, HCV localizes to the detergent-resistant membrane fraction (DRM) derived from the ER, where the viral replication and assembly take place.⁴ Thus, of the novel interactions identified in our Y2H assay, we focused on two ER-localized host factors RTN1 and RTN3 (Figure 3). RTN1 and RTN3 belong to a group of proteins named Reticulons, which are integral to maintaining the shape and organization of the

ER and have been implicated in facilitating the replication of various positive-strand RNA viruses.^{96–98} Furthermore, both RTN1 and RTN3 have been specifically detected in the very low density lipoprotein (VLDL) transport vesicle (VTV);⁹⁹ VTV is a key component of the VLDL secretory pathway, which plays an essential role in the production and the release of the infectious HCV particles.¹⁰⁰ Therefore, NSSA interactions with RTN1 and RTN3 suggested novel and potentially crucial roles of the two host proteins in the replication and/or release stages of the HCV lifecycle.

We performed cellular assays to assess the impact of RTN1 and RTN3 siRNA knockdowns on HCV replication and release. Since the HCV-production systems using the HCV JFH1 infectious strain (genotype 2a) isolates alone are capable of both efficient replication and the production of the infectious HCV particles, JFH1 was used to infect the Huh7OK1 cell line 24h after transfection with each siRNA (see Materials and Methods). The infected cells were harvested after 72 h postinfection, and the expression of each host protein was assessed by qRT-PCR (Figure 4A). The viral titer was significantly decreased by individual and double knockdowns of RTN1 and RTN3 (Figure 4B). However, RTN1 and RTN3 knockdowns had no effect on the intracellular viral RNA levels in the HCV infected cells (Figure 4C), suggesting that RTN1 and RTN3 regulate HCV propagation but not HCV replication.

CONCLUSIONS

We describe here our observations of PPIs between HCV NSSA and host proteins. By employing a multifold approach involving an experimental Y2H assay and literature mining, we derived a comprehensive set of experimentally determined binary interactions between NSSA and host proteins. We proceeded to map the combined NSSA–host interactions onto an overall interaction network, which comprised a repertoire of connections, which potentially enable NSSA to link up with and modulate the components of the host cellular networks. We then employed a network-based approach to understand the biological context of these connections in HCV pathogenesis with the help of the TargetMine data warehouse.

A functional analysis of the PPI networks highlighted NSSA interactions with several well connected host factors (hubs) and centrally located “bottlenecks” in the host cellular networks that function in cellular pathways associated with immune system and cell signaling, cellular adhesion and cell transport, cell growth and cell death and ER homeostasis among others. The “bottlenecks” include several proteins that were previously implicated in HCV pathogenesis, thereby suggesting that NSSA interactions with centrally connected host factors may enable the virus to influence strongly the host cellular processes in HCV infection. Notably, many bottlenecks were mapped to pathways associated with the infectious diseases induced by diverse bacterial and viral pathogens of the human host. These observations thus suggest the presence of some common themes underlying the onset of various human diseases associated with pathogenic infection in humans, a better understanding of which may be helpful in optimizing broad spectrum approaches to counteracting a wide range of pathogenic infections.

Cellular assays based on siRNA knockdowns in the HCV infected and replicon cells demonstrated RTN1 and RTN3, ER-localized NSSA interacting proteins, to be novel regulators of HCV propagation, but not replication, and thus promising novel candidates for anti-HCV therapy.

Our analysis therefore provides further insights into the role of NSSA–host interactions in HCV infection, a deeper understanding of which may aid in the identification of new clinically relevant targets for optimizing the therapeutic strategies to manipulate HCV–host interactions and thus more effectively combating HCV infection. Our analysis also emphasizes the importance of elaborate network-based computational approaches that integrate diverse biological data types in investigating host–pathogen interactions.

ASSOCIATED CONTENT

Supporting Information

Supporting methods, figures, and tables. This material is available free of charge via the Internet at <http://pubs.acs.org>.

AUTHOR INFORMATION

Corresponding Author

*E-mail: kenji@nibio.go.jp (K.M.); lokesh@nibio.go.jp (L.P.T.). Tel: +81-72-641-9890. Fax: +81-72-641-9881.

Author Contributions

[†]L. P. Tripathi and H. Kambara contributed equally to this work.

Notes

The authors declare no competing financial interest.

ACKNOWLEDGMENTS

This study was supported by the Industrial Technology Research Grant Program in 2007 from New Energy and Industrial Technology Development Organization (NEDO) of Japan and also by grants-in-aid from the Ministry of Health, Labor, and Welfare; the Ministry of Education, Culture, Sports, Science, and Technology; the Osaka University Global Center of Excellence Program; and the Foundation for Biomedical Research and Innovation.

REFERENCES

- (1) Dubuisson, J. Hepatitis C virus proteins. *World J. Gastroenterol.* **2007**, *13* (17), 2406–15.
- (2) Moriishi, K.; Matsuura, Y. Host factors involved in the replication of hepatitis C virus. *Rev. Med. Virol.* **2007**, *17* (5), 343–54.
- (3) Myrnel, H.; Ulvestad, E.; Asjo, B. The hepatitis C virus enigma. *APMIS* **2009**, *117* (5–6), 427–39.
- (4) Tang, H.; Grise, H. Cellular and molecular biology of HCV infection and hepatitis. *Clin. Sci.* **2009**, *117* (2), 49–65.
- (5) Pol, S.; Vallet-Pichard, A.; Corouge, M.; Mallet, V. O. Hepatitis C: epidemiology, diagnosis, natural history and therapy. *Contrib. Nephrol.* **2012**, *176*, 1–9.
- (6) Kuiken, C.; Simmonds, P. Nomenclature and numbering of the hepatitis C virus. *Methods Mol. Biol.* **2009**, *510*, 33–53.
- (7) Moradpour, D.; Penin, F.; Rice, C. M. Replication of hepatitis C virus. *Nat. Rev. Microbiol.* **2007**, *5* (6), 453–63.
- (8) Love, R. A.; Brodsky, O.; Hickey, M. J.; Wells, P. A.; Cronin, C. N. Crystal structure of a novel dimeric form of NSSA domain I protein from hepatitis C virus. *J. Virol.* **2009**, *83* (9), 4395–403.
- (9) Yamasaki, L. H.; Arcuri, H. A.; Jardim, A. C.; Bittar, C.; de Carvalho-Mello, I. M.; Rahal, P. New insights regarding HCV-NSSA structure/function and indication of genotypic differences. *Virol. J.* **2012**, *9*, 14.
- (10) Appel, N.; Zayas, M.; Miller, S.; Krijnse-Locker, J.; Schaller, T.; Friebe, P.; Kallis, S.; Engel, U.; Bartenschlager, R. Essential role of domain III of nonstructural protein 5A for hepatitis C virus infectious particle assembly. *PLoS Pathog.* **2008**, *4* (3), e1000035.

- (11) Gale, M. J., Jr.; Korth, M. J.; Tang, N. M.; Tan, S. L.; Hopkins, D. A.; Dever, T. E.; Polyak, S. J.; Gretsch, D. R.; Katze, M. G. Evidence that hepatitis C virus resistance to interferon is mediated through repression of the PKR protein kinase by the nonstructural 5A protein. *Virology* **1997**, *230* (2), 217–27.
- (12) Ghosh, S.; Ahrens, W. A.; Phatak, S. U.; Hwang, S.; Schrum, L. W.; Bonkovsky, H. L. Association of filamin A and vimentin with hepatitis C virus proteins in infected human hepatocytes. *J. Viral Hepatitis* **2011**, *18* (10), e568–77.
- (13) Gao, M.; Nettles, R. E.; Belema, M.; Snyder, L. B.; Nguyen, V. N.; Fridell, R. A.; Serrano-Wu, M. H.; Langley, D. R.; Sun, J. H.; O'Boyle, D. R., 2nd; Lemm, J. A.; Wang, C.; Knipe, J. O.; Chien, C.; Colonna, R. J.; Grasela, D. M.; Meanwell, N. A.; Hamann, L. G. Chemical genetics strategy identifies an HCV NSSA inhibitor with a potent clinical effect. *Nature* **2010**, *465* (7294), 96–100.
- (14) Lee, C. Discovery of hepatitis C virus NSSA inhibitors as a new class of anti-HCV therapy. *Arch. Pharmacol. Res.* **2011**, *34* (9), 1403–7.
- (15) Lemm, J. A.; O'Boyle, D., 2nd; Liu, M.; Nower, P. T.; Colonna, R.; Deshpande, M. S.; Snyder, L. B.; Martin, S. W.; St Laurent, D. R.; Serrano-Wu, M. H.; Romine, J. L.; Meanwell, N. A.; Gao, M. Identification of hepatitis C virus NSSA inhibitors. *J. Virol.* **2010**, *84* (1), 482–91.
- (16) Lemon, S. M.; McKeating, J. A.; Pietschmann, T.; Frick, D. N.; Glenn, J. S.; Tellinghuisen, T. L.; Symons, J.; Furman, P. A. Development of novel therapies for hepatitis C. *Antiviral Res.* **2010**, *86* (1), 79–92.
- (17) Fusco, D. N.; Chung, R. T. Novel therapies for hepatitis C: insights from the structure of the virus. *Annu. Rev. Med.* **2012**, *63*, 373–87.
- (18) Buhler, S.; Bartenschlager, R. New targets for antiviral therapy of chronic hepatitis C. *Liver Int.* **2012**, *32* (Suppl 1), 9–16.
- (19) Sarrazin, C.; Hezode, C.; Zeuzem, S.; Pawlotsky, J. M. Antiviral strategies in hepatitis C virus infection. *J. Hepatol.* **2012**, *56* (Suppl), S88–S100.
- (20) Wang, S.; Wu, X.; Pan, T.; Song, W.; Wang, Y.; Zhang, F.; Yuan, Z. Viperin inhibits hepatitis C virus replication by interfering with binding of NSSA to host protein hVAP-33. *J. Gen. Virol.* **2012**, *93* (Pt1), 83–92.
- (21) Durmus Tekir, S.; Cakir, T.; Ulgen, K. O. Infection strategies of bacterial and viral pathogens through pathogen-human protein-protein interactions. *Front. Microbiol.* **2012**, *3*, 46.
- (22) de Chasse, B.; Navratil, V.; Tafforeau, L.; Hiet, M. S.; Aublin-Gex, A.; Agaue, S.; Meiffren, G.; Pradezynski, F.; Faria, B. F.; Chantier, T.; Le Breton, M.; Pellet, J.; Davoust, N.; Mangeot, P. E.; Chaboud, A.; Penin, F.; Jacob, Y.; Vidalain, P. O.; Vidal, M.; Andre, P.; Rabourdin-Combe, C.; Lotteau, V. Hepatitis C virus infection protein network. *Mol. Syst. Biol.* **2008**, *4*, 230.
- (23) Tan, S. L.; Ganji, G.; Paepfer, B.; Proll, S.; Katze, M. G. Systems biology and the host response to viral infection. *Nat. Biotechnol.* **2007**, *25* (12), 1383–9.
- (24) Tripathi, L. P.; Kataoka, C.; Taguwa, S.; Moriishi, K.; Mori, Y.; Matsuura, Y.; Mizuguchi, K. Network based analysis of hepatitis C virus Core and NS4B protein interactions. *Mol. BioSyst.* **2010**, *6* (12), 2539–53.
- (25) Friedel, C. C.; Haas, J. Virus-host interactomes and global models of virus-infected cells. *Trends Microbiol.* **2011**, *19* (10), S01–8.
- (26) Tafforeau, L.; Rabourdin-Combe, C.; Lotteau, V. Virus-human cell interactomes. *Methods Mol. Biol.* **2012**, *812*, 103–20.
- (27) Aizaki, H.; Aoki, Y.; Harada, T.; Ishii, K.; Suzuki, T.; Nagamori, S.; Toda, G.; Matsuura, Y.; Miyamura, T. Full-length complementary DNA of hepatitis C virus genome from an infectious blood sample. *Hepatology* **1998**, *27* (2), 621–7.
- (28) Hamamoto, I.; Nishimura, Y.; Okamoto, T.; Aizaki, H.; Liu, M.; Mori, Y.; Abe, T.; Suzuki, T.; Lai, M. M.; Miyamura, T.; Moriishi, K.; Matsuura, Y. Human VAP-B is involved in hepatitis C virus replication through interaction with NSSA and NSSB. *J. Virol.* **2005**, *79* (21), 13473–82.
- (29) Rebolz-Schuhmann, D.; Kirsch, H.; Arregui, M.; Gaudan, S.; Riethoven, M.; Stoehr, P. EBIMed—text crunching to gather facts for proteins from Medline. *Bioinformatics* **2007**, *23* (2), e237–44.
- (30) Rebolz-Schuhmann, D.; Arregui, M.; Gaudan, S.; Kirsch, H.; Jimeno, A. Text processing through Web services: calling Whatizit. *Bioinformatics* **2008**, *24* (2), 296–8.
- (31) Stark, C.; Breitkreutz, B. J.; Reguly, T.; Boucher, L.; Breitkreutz, A.; Tyers, M. BioGRID: a general repository for interaction datasets. *Nucleic Acids Res.* **2006**, *34* (Database issue), D535–9.
- (32) Turner, B.; Razick, S.; Turinsky, A. L.; Vlasblom, J.; Crowdy, E. K.; Cho, E.; Morrison, K.; Donaldson, I. M.; Wodak, S. J. iRefWeb: interactive analysis of consolidated protein interaction data and their supporting evidence. *Database* **2010**, *2010*, baq023.
- (33) Chen, Y. A.; Tripathi, L. P.; Mizuguchi, K. TargetMine, an integrated data warehouse for candidate gene prioritisation and target discovery. *PLoS One* **2011**, *6* (3), e17844.
- (34) Cline, M. S.; Smoot, M.; Cerami, E.; Kuchinsky, A.; Landys, N.; Workman, C.; Christmas, R.; Avila-Campilo, I.; Creech, M.; Gross, B.; Hanspers, K.; Isserlin, R.; Kelley, R.; Killcoyne, S.; Lotia, S.; Maere, S.; Morris, J.; Ono, K.; Pavlovic, V.; Pico, A. R.; Vailaya, A.; Wang, P. L.; Adler, A.; Conklin, B. R.; Hood, L.; Kuiper, M.; Sander, C.; Schmulevich, I.; Schwikowski, B.; Warner, G. J.; Ideker, T.; Bader, G. D. Integration of biological networks and gene expression data using Cytoscape. *Nat. Protoc.* **2007**, *2* (10), 2366–82.
- (35) Smoot, M. E.; Ono, K.; Ruscheinski, J.; Wang, P. L.; Ideker, T. Cytoscape 2.8: new features for data integration and network visualization. *Bioinformatics* **2011**, *27* (3), 431–2.
- (36) Assenov, Y.; Ramirez, F.; Schelhorn, S. E.; Lengauer, T.; Albrecht, M. Computing topological parameters of biological networks. *Bioinformatics* **2008**, *24* (2), 282–4.
- (37) Lees, J.; Yeats, C.; Perkins, J.; Sillitoe, I.; Rentzsch, R.; Dessailly, B. H.; Orengo, C. Gene3D: a domain-based resource for comparative genomics, functional annotation and protein network analysis. *Nucleic Acids Res.* **2012**, *40* (Database issue), D465–71.
- (38) Ashburner, M.; Ball, C. A.; Blake, J. A.; Botstein, D.; Butler, H.; Cherry, J. M.; Davis, A. P.; Dolinski, K.; Dwight, S. S.; Eppig, J. T.; Harris, M. A.; Hill, D. P.; Issel-Tarver, L.; Kasarskis, A.; Lewis, S.; Matese, J. C.; Richardson, J. E.; Ringwald, M.; Rubin, G. M.; Sherlock, G. Gene ontology: tool for the unification of biology. The Gene Ontology Consortium. *Nat. Genet.* **2000**, *25* (1), 25–9.
- (39) Aoki-Kinoshita, K. F.; Kanehisa, M. Gene annotation and pathway mapping in KEGG. *Methods Mol. Biol.* **2007**, *396*, 71–91.
- (40) Benjamini, Y.; Hochberg, Y. Controlling the false discovery rate—A practical and powerful approach to multiple testing. *J. R. Stat. Soc. B* **1995**, *57* (1), 289–300.
- (41) Noble, W. S. How does multiple testing correction work? *Nat. Biotechnol.* **2009**, *27* (12), 1135–7.
- (42) Okamoto, K.; Mori, Y.; Komoda, Y.; Okamoto, T.; Okochi, M.; Takeda, M.; Suzuki, T.; Moriishi, K.; Matsuura, Y. Intramembrane processing by signal peptide peptidase regulates the membrane localization of hepatitis C virus core protein and viral propagation. *J. Virol.* **2008**, *82* (17), 8349–61.
- (43) Okamoto, T.; Omori, H.; Kaname, Y.; Abe, T.; Nishimura, Y.; Suzuki, T.; Miyamura, T.; Yoshimori, T.; Moriishi, K.; Matsuura, Y. A single-amino-acid mutation in hepatitis C virus NSSA disrupting FKBP8 interaction impairs viral replication. *J. Virol.* **2008**, *82* (7), 3480–9.
- (44) Wakita, T.; Pietschmann, T.; Kato, T.; Date, T.; Miyamoto, M.; Zhao, Z.; Murthy, K.; Habermann, A.; Krausslich, H. G.; Mizokami, M.; Bartenschlager, R.; Liang, T. J. Production of infectious hepatitis C virus in tissue culture from a cloned viral genome. *Nat. Med.* **2005**, *11* (7), 791–6.
- (45) Taguwa, S.; Kambara, H.; Omori, H.; Tani, H.; Abe, T.; Mori, Y.; Suzuki, T.; Yoshimori, T.; Moriishi, K.; Matsuura, Y. Co-chaperone activity of human butyrate-induced transcript 1 facilitates hepatitis C virus replication through an Hsp90-dependent pathway. *J. Virol.* **2009**, *83* (20), 10427–36.
- (46) Kukiwara, H.; Moriishi, K.; Taguwa, S.; Tani, H.; Abe, T.; Mori, Y.; Suzuki, T.; Fukuhara, T.; Taketomi, A.; Maehara, Y.; Matsuura, Y.

- Human VAP-C negatively regulates hepatitis C virus propagation. *J. Virol.* **2009**, *83* (16), 7959–69.
- (47) Nanda, S. K.; Herion, D.; Liang, T. J. The SH3 binding motif of HCV [corrected] NSSA protein interacts with Bin1 and is important for apoptosis and infectivity. *Gastroenterology* **2006**, *130* (3), 794–809.
- (48) Liu, A. W.; Cai, J.; Zhao, X. L.; Jiang, T. H.; He, T. F.; Fu, H. Q.; Zhu, M. H.; Zhang, S. H. ShRNA-targeted MAP4K4 inhibits hepatocellular carcinoma growth. *Clin. Cancer Res.* **2011**, *17* (4), 710–20.
- (49) Woodhouse, S. D.; Narayan, R.; Latham, S.; Lee, S.; Antrobus, R.; Gangadharan, B.; Luo, S.; Schroth, G. P.; Klenerman, P.; Zitzmann, N. Transcriptome sequencing, microarray, and proteomic analyses reveal cellular and metabolic impact of hepatitis C virus infection in vitro. *Hepatology* **2010**, *52* (2), 443–53.
- (50) MacPherson, J. I.; Sidders, B.; Wieland, S.; Zhong, J.; Targett-Adams, P.; Lohmann, V.; Backes, P.; Delpuech-Adams, O.; Chisari, F.; Lewis, M.; Parkinson, T.; Robertson, D. L. An integrated transcriptomic and meta-analysis of hepatoma cells reveals factors that influence susceptibility to HCV infection. *PLoS One* **2011**, *6* (10), e25584.
- (51) Yamashita, T.; Honda, M.; Kaneko, S. Molecular mechanisms of hepatocarcinogenesis in chronic hepatitis C virus infection. *J. Gastroenterol. Hepatol.* **2011**, *26* (6), 960–4.
- (52) Yu, H.; Kim, P. M.; Sprecher, E.; Trifonov, V.; Gerstein, M. The importance of bottlenecks in protein networks: correlation with gene essentiality and expression dynamics. *PLoS Comput. Biol.* **2007**, *3* (4), e59.
- (53) Rasmussen, A. L.; Diamond, D. L.; McDermott, J. E.; Gao, X.; Metz, T. O.; Matzke, M. M.; Carter, V. S.; Belisle, S. E.; Korth, M. J.; Waters, K. M.; Smith, R. D.; Katze, M. G. Systems virology identifies a mitochondrial fatty acid oxidation enzyme, dodecenoyl coenzyme A delta isomerase, required for hepatitis C virus replication and likely pathogenesis. *J. Virol.* **2011**, *85* (22), 11646–54.
- (54) Diamond, D. L.; Krasnoselsky, A. L.; Burnum, K. E.; Monroe, M. E.; Webb-Robertson, B. J.; McDermott, J. E.; Yeh, M. M.; Dzib, J. F.; Susnow, N.; Strom, S.; Proll, S. C.; Belisle, S. E.; Purdy, D. E.; Rasmussen, A. L.; Walters, K. A.; Jacobs, J. M.; Gritsenko, M. A.; Camp, D. G.; Bhattacharya, R.; Perkins, J. D.; Carithers, R. L., Jr.; Liou, I. W.; Larson, A. M.; Benecke, A.; Waters, K. M.; Smith, R. D.; Katze, M. G. Proteome and computational analyses reveal new insights into the mechanisms of hepatitis C virus-mediated liver disease posttransplantation. *Hepatology* **2012**, *56* (1), 28–38.
- (55) He, Y.; Nakao, H.; Tan, S. L.; Polyak, S. J.; Neddermann, P.; Vijaysri, S.; Jacobs, B. L.; Katze, M. G. Subversion of cell signaling pathways by hepatitis C virus nonstructural 5A protein via interaction with Grb2 and P85 phosphatidylinositol 3-kinase. *J. Virol.* **2002**, *76* (18), 9207–17.
- (56) Jiang, Y. F.; He, B.; Li, N. P.; Ma, J.; Gong, G. Z.; Zhang, M. The oncogenic role of NSSA of hepatitis C virus is mediated by up-regulation of survivin gene expression in the hepatocellular cell through p53 and NF-kappaB pathways. *Cell Biol. Int.* **2011**, *35* (12), 1225–32.
- (57) Pfannkuche, A.; Buther, K.; Karthe, J.; Poenisch, M.; Bartenschlager, R.; Trilling, M.; Hengel, H.; Willbold, D.; Haussinger, D.; Bode, J. G. c-Src is required for complex formation between the hepatitis C virus-encoded proteins NSSA and NS5B: a prerequisite for replication. *Hepatology* **2011**, *53* (4), 1127–36.
- (58) Calderwood, M. A.; Venkatesan, K.; Xing, L.; Chase, M. R.; Vazquez, A.; Holthaus, A. M.; Ewence, A. E.; Li, N.; Hirozane-Kishikawa, T.; Hill, D. E.; Vidal, M.; Kieff, E.; Johannsen, E. Epstein-Barr virus and virus human protein interaction maps. *Proc. Natl. Acad. Sci. U. S. A.* **2007**, *104* (18), 7606–11.
- (59) Pichlmair, A.; Kandasamy, K.; Alvisi, G.; Mulhern, O.; Sacco, R.; Habjan, M.; Binder, M.; Stefanovic, A.; Eberle, C. A.; Goncalves, A.; Burckstummer, T.; Muller, A. C.; Fauster, A.; Holze, C.; Lindsten, K.; Goodbourn, S.; Kochs, G.; Weber, F.; Bartenschlager, R.; Bowie, A. G.; Bennett, K. L.; Colinge, J.; Superti-Furga, G. Viral immune modulators perturb the human molecular network by common and unique strategies. *Nature* **2012**, *487* (7408), 486–90.
- (60) Huang, H.; Jedynak, B. M.; Bader, J. S. Where have all the interactions gone? Estimating the coverage of two-hybrid protein interaction maps. *PLoS Comput. Biol.* **2007**, *3* (11), e214.
- (61) Nordle Gilliver, A.; Griffin, S.; Harris, M. Identification of a novel phosphorylation site in hepatitis C virus NSSA. *J. Gen. Virol.* **2010**, *91* (Pt 10), 2428–32.
- (62) Qiu, D.; Lemm, J. A.; O’Boyle, D. R., 2nd; Sun, J. H.; Nower, P. T.; Nguyen, V.; Hamann, L. G.; Snyder, L. B.; Deon, D. H.; Ruediger, E.; Meanwell, N. A.; Belema, M.; Gao, M.; Fridell, R. A. The effects of NSSA inhibitors on NSSA phosphorylation, polyprotein processing and localization. *J. Gen. Virol.* **2011**, *92* (Pt11), 2502–11.
- (63) Tellinghuisen, T. L.; Foss, K. L.; Treadaway, J. Regulation of hepatitis C virus production via phosphorylation of the NSSA protein. *PLoS Pathog.* **2008**, *4* (3), e1000032.
- (64) Chen, K. C.; Wang, T. Y.; Chan, C. H. Associations between HIV and human pathways revealed by protein-protein interactions and correlated gene expression profiles. *PLoS One* **2012**, *7* (3), e34240.
- (65) Rozenblatt-Rosen, O.; Deo, R. C.; Padi, M.; Adelmant, G.; Calderwood, M. A.; Rolland, T.; Grace, M.; Dricot, A.; Askenazi, M.; Tavares, M.; Pevzner, S. J.; Abderazzaq, F.; Byrdson, D.; Carvunis, A. R.; Chen, A. A.; Cheng, J.; Correll, M.; Duarte, M.; Fan, C.; Feltkamp, M. C.; Ficarro, S. B.; Franchi, R.; Garg, B. K.; Gulbahce, N.; Hao, T.; Holthaus, A. M.; James, R.; Korkhin, A.; Litovchick, L.; Mar, J. C.; Pak, T. R.; Rabello, S.; Rubio, R.; Shen, Y.; Singh, S.; Spangle, J. M.; Tasan, M.; Wanamaker, S.; Webber, J. T.; Roecklein-Canfield, J.; Johannsen, E.; Barabasi, A. L.; Beroukhim, R.; Kieff, E.; Cusick, M. E.; Hill, D. E.; Munger, K.; Marto, J. A.; Quackenbush, J.; Roth, F. P.; DeCaprio, J. A.; Vidal, M. Interpreting cancer genomes using systematic host network perturbations by tumour virus proteins. *Nature* **2012**, *487* (7408), 491–5.
- (66) Barnaba, V. Hepatitis C virus infection: a “liaison a trois” amongst the virus, the host, and chronic low-level inflammation for human survival. *J. Hepatol.* **2010**, *53* (4), 752–61.
- (67) Hiroishi, K.; Ito, T.; Imawari, M. Immune responses in hepatitis C virus infection and mechanisms of hepatitis C virus persistence. *J. Gastroenterol. Hepatol.* **2008**, *23* (10), 1473–82.
- (68) Kawai, T.; Akira, S. Toll-like receptor and RIG-I-like receptor signaling. *Ann. N. Y. Acad. Sci.* **2008**, *1143*, 1–20.
- (69) Sklan, E. H.; Charuworn, P.; Pang, P. S.; Glenn, J. S. Mechanisms of HCV survival in the host. *Nat. Rev. Gastroenterol. Hepatol.* **2009**, *6* (4), 217–27.
- (70) Kang, S. M.; Won, S. J.; Lee, G. H.; Lim, Y. S.; Hwang, S. B. Modulation of interferon signaling by hepatitis C virus non-structural 5A protein: implication of genotypic difference in interferon treatment. *FEBS Lett.* **2010**, *584* (18), 4069–76.
- (71) Li, K.; Li, N. L.; Wei, D.; Pfeffer, S. R.; Fan, M.; Pfeffer, L. M. Activation of chemokine and inflammatory cytokine response in hepatitis C virus-infected hepatocytes depends on Toll-like receptor 3 sensing of hepatitis C virus double-stranded RNA intermediates. *Hepatology* **2012**, *55* (3), 666–75.
- (72) Tanaka, S.; Arii, S. Molecularly targeted therapy for hepatocellular carcinoma. *Cancer Sci.* **2009**, *100* (1), 1–8.
- (73) Tanaka, S.; Arii, S. Current status of molecularly targeted therapy for hepatocellular carcinoma: basic science. *Int. J. Clin. Oncol.* **2010**, *15* (3), 235–41.
- (74) Villanueva, A.; Chiang, D. Y.; Newell, P.; Peix, J.; Thung, S.; Alsinet, C.; Tovar, V.; Roayaie, S.; Minguez, B.; Sole, M.; Battiston, C.; Van Laarhoven, S.; Fiel, M. I.; Di Feo, A.; Hoshida, Y.; Yea, S.; Toffanin, S.; Ramos, A.; Martignetti, J. A.; Mazzaferro, V.; Bruix, J.; Waxman, S.; Schwartz, M.; Meyerson, M.; Friedman, S. L.; Llovet, J. M. Pivotal role of mTOR signaling in hepatocellular carcinoma. *Gastroenterology* **2008**, *135* (6), 1972–83.
- (75) Cheng, D.; Zhao, L.; Zhang, L.; Jiang, Y.; Tian, Y.; Xiao, X.; Gong, G. p53 controls hepatitis C virus non-structural protein 5A-mediated downregulation of GADD45alpha expression via the NF-kappaB and PI3K-Akt pathways. *J. Gen. Virol.* **2013**, *94* (Pt 2), 326–35.
- (76) Tripathi, L. P.; Kambara, H.; Moriishi, K.; Morita, E.; Abe, T.; Mori, Y.; Chen, Y. A.; Matsuura, Y.; Mizuguchi, K. Proteomic analysis

of hepatitis C virus (HCV) core protein transfection and host regulator PA28gamma knockout in HCV pathogenesis: a network-based study. *J. Proteome Res.* **2012**, *11* (7), 3664–79.

(77) Zhao, L. J.; Zhao, P.; Chen, Q. L.; Ren, H.; Pan, W.; Qi, Z. T. Mitogen-activated protein kinase signalling pathways triggered by the hepatitis C virus envelope protein E2: implications for the prevention of infection. *Cell Proliferation* **2007**, *40* (4), 508–21.

(78) Basaranoglu, M.; Basaranoglu, G. Pathophysiology of insulin resistance and steatosis in patients with chronic viral hepatitis. *World J. Gastroenterol.* **2011**, *17* (36), 4055–62.

(79) Del Campo, J. A.; Romero-Gomez, M. Steatosis and insulin resistance in hepatitis C: a way out for the virus? *World J. Gastroenterol.* **2009**, *15* (40), 5014–9.

(80) Douglas, M. W.; George, J. Molecular mechanisms of insulin resistance in chronic hepatitis C. *World J. Gastroenterol.* **2009**, *15* (35), 4356–64.

(81) Das, G. C.; Hollinger, F. B. Molecular pathways for glucose homeostasis, insulin signaling and autophagy in hepatitis C virus induced insulin resistance in a cellular model. *Virology* **2012**, *434* (1), 5–17.

(82) Miyamoto, H.; Moriishi, K.; Moriya, K.; Murata, S.; Tanaka, K.; Suzuki, T.; Miyamura, T.; Koike, K.; Matsuura, Y. Involvement of the PA28gamma-dependent pathway in insulin resistance induced by hepatitis C virus core protein. *J. Virol.* **2007**, *81* (4), 1727–35.

(83) Kaneko, K.; Ueki, K.; Takahashi, N.; Hashimoto, S.; Okamoto, M.; Awazawa, M.; Okazaki, Y.; Ohsugi, M.; Inabe, K.; Umehara, T.; Yoshida, M.; Kakei, M.; Kitamura, T.; Luo, J.; Kulkarni, R. N.; Kahn, C. R.; Kasai, H.; Cantley, L. C.; Kadowaki, T. Class IA phosphatidylinositol 3-kinase in pancreatic beta cells controls insulin secretion by multiple mechanisms. *Cell Metab.* **2010**, *12* (6), 619–32.

(84) Milward, A.; Mankouri, J.; Harris, M. Hepatitis C virus NSSA protein interacts with beta-catenin and stimulates its transcriptional activity in a phosphoinositide-3 kinase-dependent fashion. *J. Gen. Virol.* **2010**, *91* (Pt 2), 373–81.

(85) Alberstein, M.; Zornitzki, T.; Zick, Y.; Knobler, H. Hepatitis C core protein impairs insulin downstream signalling and regulatory role of IGFBP-1 expression. *J. Viral Hepatitis* **2012**, *19* (1), 65–71.

(86) Benedicto, I.; Molina-Jimenez, F.; Bartosch, B.; Cosset, F. L.; Lavillette, D.; Prieto, J.; Moreno-Otero, R.; Valenzuela-Fernandez, A.; Aldabe, R.; Lopez-Cabrera, M.; Majano, P. L. The tight junction-associated protein occludin is required for a postbinding step in hepatitis C virus entry and infection. *J. Virol.* **2009**, *83* (16), 8012–20.

(87) Carloni, G.; Crema, A.; Valli, M. B.; Ponzetto, A.; Clementi, M. HCV infection by cell-to-cell transmission: choice or necessity? *Curr. Mol. Med.* **2012**, *12* (1), 83–95.

(88) Wilson, G. K.; Brimacombe, C. L.; Rowe, I. A.; Reynolds, G. M.; Fletcher, N. F.; Stamatakis, Z.; Bhogal, R. H.; Simoes, M. L.; Ashcroft, M.; Afford, S. C.; Mitry, R. R.; Dhawan, A.; Mee, C. J.; Hubscher, S. G.; Balfe, P.; McKeating, J. A. A dual role for hypoxia inducible factor-1alpha in the hepatitis C virus lifecycle and hepatoma migration. *J. Hepatol.* **2012**, *56* (4), 803–9.

(89) Daugherty, R. L.; Gottardi, C. J. Phospho-regulation of beta-catenin adhesion and signaling functions. *Physiology* **2007**, *22*, 303–9.

(90) Presser, L. D.; Haskett, A.; Waris, G. Hepatitis C virus-induced furin and thrombospondin-1 activate TGF-beta1: role of TGF-beta1 in HCV replication. *Virology* **2011**, *412* (2), 284–96.

(91) Berger, K. L.; Cooper, J. D.; Heaton, N. S.; Yoon, R.; Oakland, T. E.; Jordan, T. X.; Mateu, G.; Grakoui, A.; Randall, G. Roles for endocytic trafficking and phosphatidylinositol 4-kinase III alpha in hepatitis C virus replication. *Proc. Natl. Acad. Sci. U. S. A.* **2009**, *106* (18), 7577–82.

(92) Katsarou, K.; Lavdas, A. A.; Tsitoura, P.; Serti, E.; Markoulatos, P.; Mavromara, P.; Georgopoulou, U. Endocytosis of hepatitis C virus non-enveloped capsid-like particles induces MAPK-ERK1/2 signaling events. *Cell. Mol. Life Sci.* **2010**, *67*, 2491–506.

(93) Mankouri, J.; Griffin, S.; Harris, M. The hepatitis C virus non-structural protein NSSA alters the trafficking profile of the epidermal growth factor receptor. *Traffic* **2008**, *9* (9), 1497–509.

(94) Diao, J.; Pantua, H.; Ngu, H.; Komuves, L.; Diehl, L.; Schaefer, G.; Kapadia, S. B. Hepatitis C virus (HCV) induces epidermal growth factor receptor (EGFR) activation via CD81 binding for viral internalization and entry. *J. Virol.* **2012**, *86* (20), 10935–49.

(95) Yoon, H. Y.; Kales, S. C.; Luo, R.; Lipkowitz, S.; Randazzo, P. A. ARAP1 association with CIN85 affects epidermal growth factor receptor endocytic trafficking. *Biol. Cell* **2011**, *103* (4), 171–84.

(96) Katsarou, K.; Lavdas, A. A.; Tsitoura, P.; Serti, E.; Markoulatos, P.; Mavromara, P.; Georgopoulou, U. Endocytosis of hepatitis C virus non-enveloped capsid-like particles induces MAPK-ERK1/2 signaling events. *Cell. Mol. Life Sci.* **2010**, *67* (14), 2491–506.

(97) Diaz, A.; Ahlquist, P. Role of host reticulon proteins in rearranging membranes for positive-strand RNA virus replication. *Curr. Opin. Microbiol.* **2012**, *15* (4), 519–24.

(98) Diaz, A.; Wang, X.; Ahlquist, P. Membrane-shaping host reticulon proteins play crucial roles in viral RNA replication compartment formation and function. *Proc. Natl. Acad. Sci. U. S. A.* **2010**, *107* (37), 16291–6.

(99) Rahim, A.; Nafi-valencia, E.; Siddiqi, S.; Basha, R.; Runyon, C. C.; Siddiqi, S. A. Proteomic analysis of the very low density lipoprotein (VLDL) transport vesicles. *J. Proteomics* **2012**, *75* (7), 2225–35.

(100) Coller, K. E.; Heaton, N. S.; Berger, K. L.; Cooper, J. D.; Saunders, J. L.; Randall, G. Molecular determinants and dynamics of hepatitis C virus secretion. *PLoS Pathog.* **2012**, *8* (1), e1002466.

(101) Lai, C. K.; Jeng, K. S.; Machida, K.; Lai, M. M. Association of hepatitis C virus replication complexes with microtubules and actin filaments is dependent on the interaction of NS3 and NSSA. *J. Virol.* **2008**, *82* (17), 8838–48.

(102) Randall, G.; Panis, M.; Cooper, J. D.; Tellinghuisen, T. L.; Sukhodolets, K. E.; Pfeffer, S.; Landthaler, M.; Landgraf, P.; Kan, S.; Lindenbach, B. D.; Chien, M.; Weir, D. B.; Russo, J. J.; Ju, J.; Brownstein, M. J.; Sheridan, R.; Sander, C.; Zavolan, M.; Tuschl, T.; Rice, C. M. Cellular cofactors affecting hepatitis C virus infection and replication. *Proc. Natl. Acad. Sci. U. S. A.* **2007**, *104* (31), 12884–9.

(103) Saxena, V.; Lai, C. K.; Chao, T. C.; Jeng, K. S.; Lai, M. M. Annexin A2 is involved in the formation of hepatitis C virus replication complex on the lipid raft. *J. Virol.* **2012**, *86* (8), 4139–50.

(104) Quintavalle, M.; Sambucini, S.; Summa, V.; Orsatti, L.; Talamo, F.; De Francesco, R.; Neddermann, P. Hepatitis C virus NSSA is a direct substrate of casein kinase I-alpha, a cellular kinase identified by inhibitor affinity chromatography using specific NSSA hyperphosphorylation inhibitors. *J. Biol. Chem.* **2007**, *282* (8), 5536–44.

(105) Ivanov, A. V.; Tunitskaya, V. L.; Ivanova, O. N.; Mitkevich, V. A.; Prassolov, V. S.; Makarov, A. A.; Kukhanova, M. K.; Kochetkov, S. N. Hepatitis C virus NSSA protein modulates template selection by the RNA polymerase in in vitro system. *FEBS Lett.* **2009**, *583* (2), 277–80.

(106) Park, C. Y.; Choi, S. H.; Kang, S. M.; Kang, J. I.; Ahn, B. Y.; Kim, H.; Jung, G.; Choi, K. Y.; Hwang, S. B. Nonstructural 5A protein activates beta-catenin signaling cascades: implication of hepatitis C virus-induced liver pathogenesis. *J. Hepatol.* **2009**, *51* (5), 853–64.

(107) Zhang, Z.; Harris, D.; Pandey, V. N. The FUSE binding protein is a cellular factor required for efficient replication of hepatitis C virus. *J. Virol.* **2008**, *82* (12), 5761–73.

(108) Chen, Y. J.; Chen, Y. H.; Chow, L. P.; Tsai, Y. H.; Chen, P. H.; Huang, C. Y.; Chen, W. T.; Hwang, L. H. Heat shock protein 72 is associated with the hepatitis C virus replicase complex and enhances viral RNA replication. *J. Biol. Chem.* **2010**, *285* (36), 28183–90.

(109) Choi, Y. W.; Tan, Y. J.; Lim, S. G.; Hong, W.; Goh, P. Y. Proteomic approach identifies HSP27 as an interacting partner of the hepatitis C virus NSSA protein. *Biochem. Biophys. Res. Commun.* **2004**, *318* (2), 514–9.

(110) Ahn, J.; Chung, K. S.; Kim, D. U.; Won, M.; Kim, L.; Kim, K. S.; Nam, M.; Choi, S. J.; Kim, H. C.; Yoon, M.; Chae, S. K.; Hoe, K. L. Systematic identification of hepatocellular proteins interacting with NSSA of the hepatitis C virus. *J. Biochem. Mol. Biol.* **2004**, *37* (6), 741–8.

- (111) Amako, Y.; Sarkeshik, A.; Hotta, H.; Yates, J., 3rd; Siddiqui, A. Role of oxysterol binding protein in hepatitis C virus infection. *J. Virol.* **2009**, *83* (18), 9237–46.
- (112) Lim, Y. S.; Tran, H. T.; Park, S. J.; Yim, S. A.; Hwang, S. B. Peptidyl-prolyl isomerase Pin1 is a cellular factor required for hepatitis C virus propagation. *J. Virol.* **2011**, *85* (17), 8777–88.
- (113) Chen, Y. C.; Su, W. C.; Huang, J. Y.; Chao, T. C.; Jeng, K. S.; Machida, K.; Lai, M. M. Polo-like kinase 1 is involved in hepatitis C virus replication by hyperphosphorylating NSSA. *J. Virol.* **2010**, *84* (16), 7983–93.
- (114) Waller, H.; Chatterji, U.; Gallay, P.; Parkinson, T.; Targett-Adams, P. The use of AlphaLISA technology to detect interaction between hepatitis C virus-encoded NSSA and cyclophilin A. *J. Virol. Methods* **2010**, *165* (2), 202–10.
- (115) Chatterji, U.; Lim, P.; Bobardt, M. D.; Wieland, S.; Cordek, D. G.; Vuagniaux, G.; Chisari, F.; Cameron, C. E.; Targett-Adams, P.; Parkinson, T.; Gallay, P. A. HCV resistance to cyclosporin A does not correlate with a resistance of the NSSA-cyclophilin A interaction to cyclophilin inhibitors. *J. Hepatol.* **2010**, *53* (1), 50–6.
- (116) Georgopoulou, U.; Tsitoura, P.; Kalamvoki, M.; Mavromara, P. The protein phosphatase 2A represents a novel cellular target for hepatitis C virus NSSA protein. *Biochimie* **2006**, *88* (6), 651–62.
- (117) Helbig, K. J.; Eyre, N. S.; Yip, E.; Narayana, S.; Li, K.; Fiches, G.; McCartney, E. M.; Jangra, R. K.; Lemon, S. M.; Beard, M. R. The antiviral protein viperin inhibits hepatitis C virus replication via interaction with nonstructural protein 5A. *Hepatology* **2011**, *54* (5), 1506–17.
- (118) Kumthip, K.; Chusri, P.; Jilg, N.; Zhao, L.; Fusco, D. N.; Zhao, H.; Goto, K.; Cheng, D.; Schaefer, E. A.; Zhang, L.; Pantip, C.; Thongsawat, S.; O'Brien, A.; Peng, L. F.; Maneekarn, N.; Chung, R. T.; Lin, W. Hepatitis C virus NSSA disrupts STAT1 phosphorylation and suppresses type I interferon signaling. *J. Virol.* **2012**, *86* (16), 8581–91.
- (119) Inubushi, S.; Nagano-Fujii, M.; Kitayama, K.; Tanaka, M.; An, C.; Yokozaki, H.; Yamamura, H.; Nuriya, H.; Kohara, M.; Sada, K.; Hotta, H. Hepatitis C virus NSSA protein interacts with and negatively regulates the non-receptor protein tyrosine kinase Syk. *J. Gen. Virol.* **2008**, *89* (Pt 5), 1231–42.



Contents lists available at ScienceDirect

Biochemical and Biophysical Research Communications

journal homepage: www.elsevier.com/locate/ybbrc

A novel TK-NOG based humanized mouse model for the study of HBV and HCV infections



Keiichi Kosaka^{a,b}, Nobuhiko Hiraga^{a,b}, Michio Imamura^{a,b}, Satoshi Yoshimi^{a,b}, Eisuke Murakami^{a,b}, Takashi Nakahara^{a,b}, Yoji Honda^{a,b}, Atsushi Ono^{a,b}, Tomokazu Kawaoka^{a,b}, Masataka Tsuge^{a,b}, Hiromi Abe^{a,b}, C. Nelson Hayes^{a,b,c}, Daiki Miki^{b,c}, Hiroshi Aikata^{a,b}, Hidenori Ochi^{b,c}, Yuji Ishida^{b,d}, Chise Tateno^{b,d}, Katsutoshi Yoshizato^{b,d}, Tamito Sasaki^{a,b}, Kazuaki Chayama^{a,b,c,*}

^a Department of Gastroenterology and Metabolism, Applied Life Sciences, Institute of Biomedical & Health Science, Hiroshima University, Hiroshima, Japan

^b Liver Research Project Center, Hiroshima University, Hiroshima, Japan

^c Laboratory for Digestive Diseases, Center for Genomic Medicine, The Institute of Physical and Chemical Research (RIKEN), Hiroshima, Japan

^d PhoenixBio Co., Ltd., Higashihiroshima, Japan

ARTICLE INFO

Article history:

Received 20 September 2013

Available online 16 October 2013

Keywords:

Human hepatocyte chimeric mouse

TK-NOG mouse

uPA-SCID mouse

Hepatitis B virus

Hepatitis C virus

Human serum albumin

ABSTRACT

The immunodeficient mice transplanted with human hepatocytes are available for the study of the human hepatitis viruses. Recently, human hepatocytes were also successfully transplanted in herpes simplex virus type-1 thymidine kinase (TK)-NOG mice. In this study, we attempted to infect hepatitis virus in humanized TK-NOG mice and urokinase-type plasminogen activator-severe combined immunodeficiency (uPA-SCID) mice. TK-NOG mice were injected intraperitoneally with 6 mg/kg of ganciclovir (GCV), and transplanted with human hepatocytes. Humanized TK-NOG mice and uPA/SCID mice were injected with hepatitis B virus (HBV)- or hepatitis C virus (HCV)-positive human serum samples. Human hepatocyte repopulation index (RI) estimated from human serum albumin levels in TK-NOG mice correlated well with pre-transplantation serum ALT levels induced by ganciclovir treatment. All humanized TK-NOG and uPA-SCID mice injected with HBV infected serum developed viremia irrespective of lower replacement index. In contrast, establishment of HCV viremia was significantly more frequent in TK-NOG mice with low human hepatocyte RI (<70%) than uPA-SCID mice with similar RI. Frequency of mice spontaneously in early stage of viral infection experiment (8 weeks after injection) was similar in both TK-NOG mice and uPA-SCID mice. Effects of drug treatment with entecavir or interferon were similar in both mouse models. TK-NOG mice thus useful for study of hepatitis virus virology and evaluation of anti-viral drugs.

© 2013 Elsevier Inc. All rights reserved.

1. Introduction

Hepatitis B virus (HBV) and hepatitis C virus (HCV) infections are serious health problems worldwide. More than 350 and 170 million people are infected with HBV and HCV, respectively [1,2]. Both types of hepatitis viruses result in the development

of chronic liver infection and potentially death due to liver failure and hepatocellular carcinoma [3]. Although the chimpanzee is a useful animal model for the study of HBV and HCV infection, there are ethical restrictions and hampered by the high financial cost on the use of this animal. The immunodeficient mice with a urokinase-type plasminogen activator (uPA) transgene [4,5] or a targeted disruption of the murine fumaryl acetoacetate hydrolase (FAH) [6–10] were shown to be excellent recipients for human hepatocyte. These small animal models are available for hepatitis viruses infection [4,11], and are useful for the study of HBV and HCV biology [12–14]. However, there are disadvantages that limit the utility of this model for many applications, including excessive mortality [9].

Recently, human hepatocytes were successfully transplanted into severely immunodeficient NOG mice with the herpes simplex virus type-1 thymidine kinase (HSVtk) expressing in mouse hepatocytes (TK-NOG) [15]. Mouse liver cells expressing HSVtk

Abbreviations: ALT, alanine aminotransferase; GCV, ganciclovir; HBV, hepatitis B virus; HCV, hepatitis C virus; HSA, human serum albumin; HSVtk, herpes simplex virus type-1 thymidine kinase; IFN, interferon; PegIFN-alpha, pegylated interferon-alpha; RI, repopulation index; RT-PCR, reverse transcript-polymerase chain reaction; SCID, severe combined immunodeficiency; uPA, urokinase-type plasminogen activator.

* Corresponding author. Address: Department of Gastroenterology and Metabolism, Applied Life Sciences, Institute of Biomedical & Health Sciences, Hiroshima University, 1-2-3 Kasumi, Minami-ku, Hiroshima 734-8551, Japan. Fax: +81 82 255 6220.

E-mail address: chayama@hiroshima-u.ac.jp (K. Chayama).

0006-291X/\$ - see front matter © 2013 Elsevier Inc. All rights reserved.

<http://dx.doi.org/10.1016/j.bbrc.2013.10.040>

were ablated after a brief exposure to ganciclovir (GCV), and transplanted human hepatocytes were stably maintained within the mouse liver without exogenous drug administration [15]. The analyses of drug interactions and pharmacokinetics have previously been reported using TK-NOG mice transplanted with human hepatocytes [15–18]. In the present study, we succeeded in infecting human hepatocyte-transplanted TK-NOG mice with HBV and HCV and showed that this mouse model is as useful as the uPA/SCID model for the study of hepatitis viruses.

2. Materials and methods

2.1. Animal treatment

TK-NOG mice were purchased from Central Institute for Experimental Animals (CIEA, Kawasaki, Japan). Eight-week-old mice were injected intraperitoneally with 6 mg/kg of GCV twice a day. After two days, mice were re-injected with the same amount of GCV. Seven days after 1st GCV injection, mice were transplanted with 1 or 2×10^6 of human hepatocytes obtained from human hepatocyte transplanted uPA–SCID chimeric mice by collagenase perfusion method by intra-splenic injection. Transplanted human hepatocytes used in this study were obtained from a same donor. One week after the first GCV treatment, serum alanine aminotransferase (ALT) levels were measured (Fuji DRI-CHEM, Fuji Film, Tokyo, Japan). Infection, extraction of serum samples, and sacrifice were performed under ether anesthesia. Mouse serum concentration of human serum albumin (HSA), which correlated with the human hepatocyte repopulation index (RI) [15], was measured as previously described [5]. Generation of the uPA/SCID mice and transplantation of human hepatocytes were performed as described previously [5,12,19]. The experimental protocol was approved by the Ethics Review Committee for Animal Experimentation of the Graduate School of Biomedical Sciences, Hiroshima University.

2.2. Human serum samples

Human serum samples containing high titers of either genotype C HBV (5.3×10^6 copies/mL) or genotype 1b HCV (2.2×10^6 copies/mL) were obtained from patients with chronic hepatitis who provided written informed consent. The individual serum samples were divided into small aliquots and stored separately in liquid nitrogen until use. Mice were injected intravenously with 50 μ L of either HBV- or HCV-positive human serum. The study protocol conforms to the ethical guidelines of the 1975 Declaration of Helsinki and was approved a priori by the institutional review committee.

2.3. Quantitation of HBV and HCV

DNA and RNA extraction and quantitation of HBV and HCV by real-time polymerase chain reaction (RT-PCR) were performed as described previously [12,13,19]. Briefly, DNA was extracted using SMITEST (Genome Science Laboratories, Tokyo, Japan) and dissolved in 20 μ L H₂O, and RNA was extracted from serum samples using SepaGene RVR (Sankojunyaku, Tokyo, Japan) and reverse transcribed with a random hexamer and a reverse transcriptase (ReverTraAce; TOYOBO, Osaka, Japan) according to the instructions provided by the manufacturer. Quantitation of HBV DNA and HCV RNA was performed using Light Cycler (Roche Diagnostic, Japan, Tokyo). The lower detection limits of real-time PCR for HBV DNA and HCV RNA are 4.4 and 3.5 log copies/mL, respectively.

2.4. Histochemical analysis of mouse liver

Liver specimens of HBV-infected TK-NOG mice were fixed with 10% buffered-paraformaldehyde and embedded in paraffin blocks for histological examination. Hematoxylin-eosin and immunohistochemical staining using antibodies against HSA (Bethyl Laboratories Inc., Montgomery, TX) and hepatitis B core antigen (HBc-Ag) (DAKO Diagnostika, Hamburg, Germany) were performed as described previously [12].

2.5. Treatment with antiviral agents

Mice were treated with antiviral agents eight weeks after HBV or HCV infection, by which time stable viremia had developed. HBV-infected mice were administered either food containing 0.3 mg of entecavir/kg of body weight/day or daily intramuscular injections with 7000 IU/kg of IFN- α (Otsuka Pharmaceutical Co., Ltd., Tokyo, Japan). HCV-infected mice were administered intramuscular injection with either 1000 IU/kg of IFN- α daily or 10 μ g/kg of PegIFN- α -2a (Chugai Pharmaceutical Co., Ltd., Tokyo, Japan) twice a week for three weeks.

2.6. Statistical analysis

Differences in HSA levels between TK-NOG mice and uPA–SCID mice, and incidence of infection between highly and poorly repopulated mice were examined for statistical significance using the Mann–Whitney *U*-test.

3. Results

3.1. Correlation between serum ALT level after GCV administration and the human hepatocyte index in TK-NOG mice

We analyzed the correlation between serum ALT levels after GCV injection and the human hepatocyte RI using 194 TK-NOG mice. Seven days after GCV injection when serum ALT levels had reached maximum levels [15], mice were transplanted with human hepatocytes. After transplantation of human hepatocytes, serum concentrations of HSA increased and reached plateau at 6–8 weeks. Serum ALT levels one week after GCV administration and HSA levels 8 weeks after hepatocyte transplantation showed a positive correlation, indicating that the higher serum ALT level, the higher the RI (Fig. 1A). HSA levels 8 weeks after human hepatocyte transplantation in TK-NOG mice were lower than in uPA–SCID mice (Fig. 1B), which indicates that mice livers were more efficiently replaced with human hepatocytes in uPA–SCID mice than in TK-NOG mice.

3.2. Infection with hepatitis viruses in humanized TK-NOG mice and uPA–SCID mice

Eight weeks after human hepatocyte transplantation, TK-NOG mice and uPA–SCID mice with HSA levels over 1.0 mg/mL were inoculated with either HBV- or HCV-positive human serum samples. Eight weeks after injection, the frequency of the development of viremia was compared between the mice with lower (<70%) and higher (\geq 70%) human hepatocyte RI. 70% of RI corresponds to 5.4 and 6.3 mg/dl of serum HAS in TK-NOG mice and uPA–SCID mice, respectively [5,15]. All humanized TK-NOG and uPA–SCID mice inoculated with HBV developed viremia 8 weeks after injection, irrespective of the RI (Fig. 2A). Incidence of HCV viremia was also high in TK-NOG mice regardless of the RI. In contrast, the frequency of HCV viremia was much lower in uPA–SCID mice with the RI. Only 20% (1 of 5) of uPA–SCID mice with low RI became

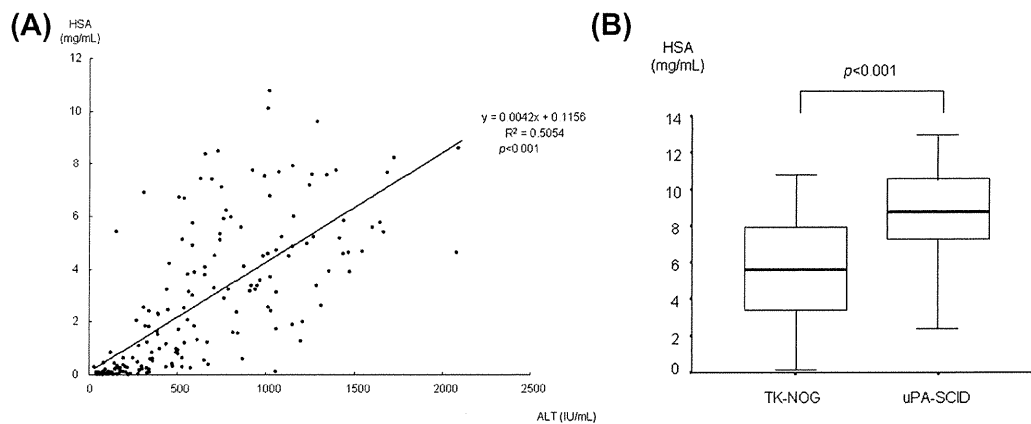


Fig. 1. Human hepatocyte repopulation index in humanized mice. Serum alaninaminotransferase (ALT) levels in TK-NOG mice were measured one week after ganciclovir treatment. Human serum albumin (HSA) levels were measured eight weeks after transplantation of human hepatocytes. (A) Correlation between serum ALT level after ganciclovir administration and human hepatocyte repopulation index in TK-NOG mice. Points represent single mouse measurements. r (Spearman rank) and P value are shown. (B) HSA levels in TK-NOG mice and uPA-SCID mice. In these box-and-whisker plots, lines within the boxes represent median values; the upper and lower lines of the boxes represent the 25th and 75th percentiles, respectively; and the upper and lower bars outside the boxes represent the 90th and 10th percentiles, respectively.

positive for HCV, whereas 94.3% (50 of 53) of mice with high RI became positive ($p = 1.07 \times 10^{-6}$). Serum viral titers gradually increased in mice that developed viremia. Eight weeks after infection, HBV DNA and HCV RNA titers increased to approximately 8 and 6 log copies/mL, respectively in both TK-NOG and uPA-SCID mice (Fig. 2B). Viremia levels were slightly higher in uPA-SCID mice than TK-NOG mice, probably due to higher human hepatocyte RI (HSA levels) in uPA-SCID mice. In HBV-infected TK-NOG mice, histological analysis showed that hepatocytes positive for HSA were also positive for HB core antigen (Fig. 2C), which is in line with our previous findings using uPA-SCID mice [12].

3.3. The effect of antiviral agents on hepatitis virus-infected humanized mice

We analyzed the effect of antiviral agents on HBV- and HCV-infected humanized mice. Eight weeks after HBV-infection, 2 humanized TK-NOG mice were orally administrated 0.3 mg/kg day of entecavir, and 2 other mice received intramuscular injections with 7000 IU/g of IFN-alpha daily for 3 weeks. Both treatments resulted in a rapid reduction of mouse serum HBV DNA titers (Fig. 3A). Two HCV-infected humanized TK-NOG mice were administrated IFN-alpha daily, and 2 other mice received PegIFN-alpha-2a injections twice a week for 3 weeks. Both treatments resulted in a reduction of HCV RNA titers in mouse serum. The effects of these antiviral agents on HBV and HCV in TK-NOG mice were similar to those in uPA-SCID mice (Fig. 3B).

3.4. Incidence of unexpected death

The incidence of unexpected death is high in human hepatocyte chimeric uPA-SCID mice [20]. Incidence of unexpected death in the early stages of viral infection (within 8 weeks of viral infection) was similar between TK-NOG mice and uPA-SCID mice (6.3% vs 10.6%, $p = 0.465$) (Fig. 4).

4. Discussion

Human hepatocyte chimeric mice are valuable tool for hepatitis virology and drug assessment [12–14]. To establish human hepatocyte chimerism, two conditions are necessary: immunodeficiency and mouse-specific liver cell damage. For immune

deficiency, SCID mice [4,5,12–14,20], NOG mice [8,21] and RAG-2 deficient mice [6,9,10] have been reported. We previously reported that the level of immunodeficiency in SCID mice, which are the most weakly immunodeficient of the three types, is sufficient to prevent rejection of transplanted human hepatocytes [5]. However, preventive treatments for human liver cell rejection via mice NK cells, such as an anti-asialo GM1 antibody, are necessary in SCID mice [5].

To evoke mouse liver cell injury, uPA and FAH transgene techniques were used [4–10]. Recently, successful human liver cell transplantation to TK-NOG mice in the absence of ongoing drug treatment after a brief exposure to a non-toxic dose of GCV has been reported [15]. We thus attempted to use TK-NOG mice to establish high levels of replacement with human hepatocytes and tried to infect hepatitis viruses.

In this study, we transplanted human hepatocytes to 194 TK-NOG mice and analyzed whether elevated serum ALT levels, which results from liver damage caused by GCV exposure, reflects HSA levels, as it is known that HSA levels are correlated with the human hepatocyte RI and can serve as a surrogate measure [15]. We found a positive correlation between ALT and HSA levels (Fig. 1A), indicating that higher levels of liver damage are associated with establishment of higher levels of repopulation of the liver with human hepatocytes. As the human hepatocyte RI obtained in this study using TK-NOG mice is lower than in uPA-SCID mice (Fig 1B), dose escalation of GCV or alternative treatment timing might result in more highly repopulated mice.

We infected humanized TK-NOG mice with hepatitis viruses and compared infection rates and serum viral titers with humanized uPA-SCID mice. HBV inoculation resulted in development of viremia without regard for the human hepatocyte replacement index in both TK-NOG mice and uPA-SCID mice (Fig. 2A). Incidence of HCV viremia was also high in TK-NOG mice regardless of HSA levels, whereas HCV viremia was infrequent in uPA-SCID mice with low HSA levels. These results are consistent with those of Vanwolleghem et al. [20] who showed, using a large number of human hepatocyte chimeric uPA-SCID mice, that an HSA level well above 1 mg/mL is important for successful HCV infection. The reason for the higher infection rate in TK-NOG mice with low human hepatocyte RI in this study is unknown. Although the level of immunodeficiency is higher in TK-NOG mice, it is difficult to conclude that this difference in immunodeficiency alone is responsible for the enhanced HCV infection rate. Although some studies have

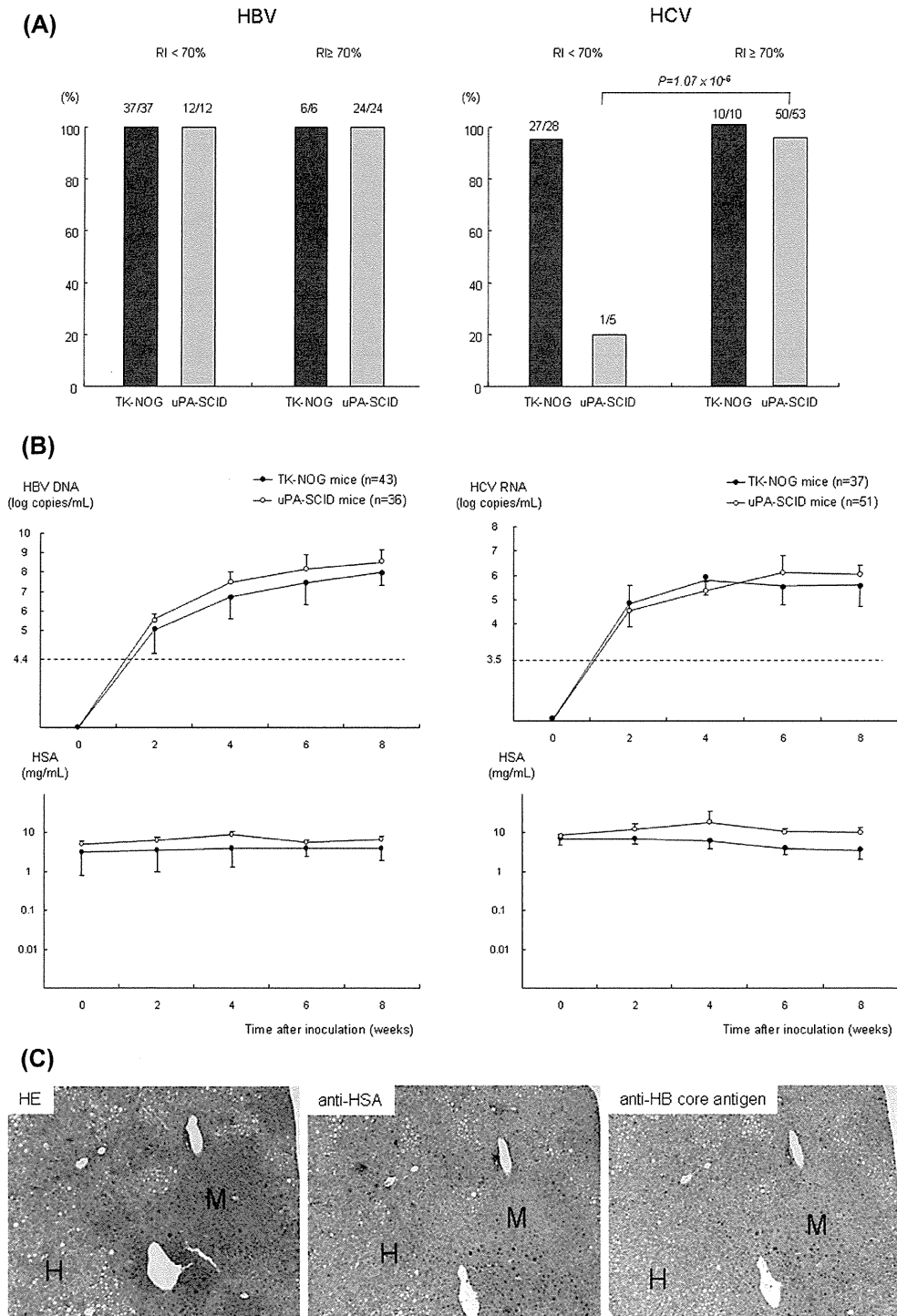


Fig. 2. Hepatitis viruses infection in chimeric mice. (A) Eight weeks after human hepatocyte transplantation, mice with serum HSA level over 1 mg/mL were inoculated with HBV- or HCV-positive human serum samples. Percentages of mice that became positive for HBV DNA (left panel) or HCV RNA (right panel) 8 weeks after inoculation according to human hepatocyte repopulation index (RI) in TK-NOG mice and uPA-SCID mice are shown. 70% of RI corresponds to 5.4 and 6.3 mg/dl of serum HSA in TK-NOG mice and uPA-SCID mice, respectively. (B) Changes in serum titers of HBV DNA (left panel) and HCV RNA (right panel) (upper panels) and HSA levels (lower panels) of TK-NOG mice and uPA-SCID mice, respectively. The horizontal dashed lines represent the lower detection limit of HBV DNA and HCV RNA (4.4 and 3.5 log copies/mL, respectively). (C) Histochemical analysis of liver samples obtained from HBV-infected TK-NOG mice. Hematoxylin-eosin staining (HE) and immunohistochemical staining using monoclonal antibodies against HSA and HB core antigen are shown. Regions are shown as human (H) and mouse (M) hepatocytes, respectively (Original magnification 100×).

reported structural differences between wild type and chimeric mice [22,23], the influence of such structural differences on HCV infectivity remains to be determined.

Human hepatocyte transplanted uPA-SCID mice are useful for evaluating antiviral agents [12–14]. In this study, we analyzed the efficacy of antiviral agents such as entecavir, IFN-alpha and

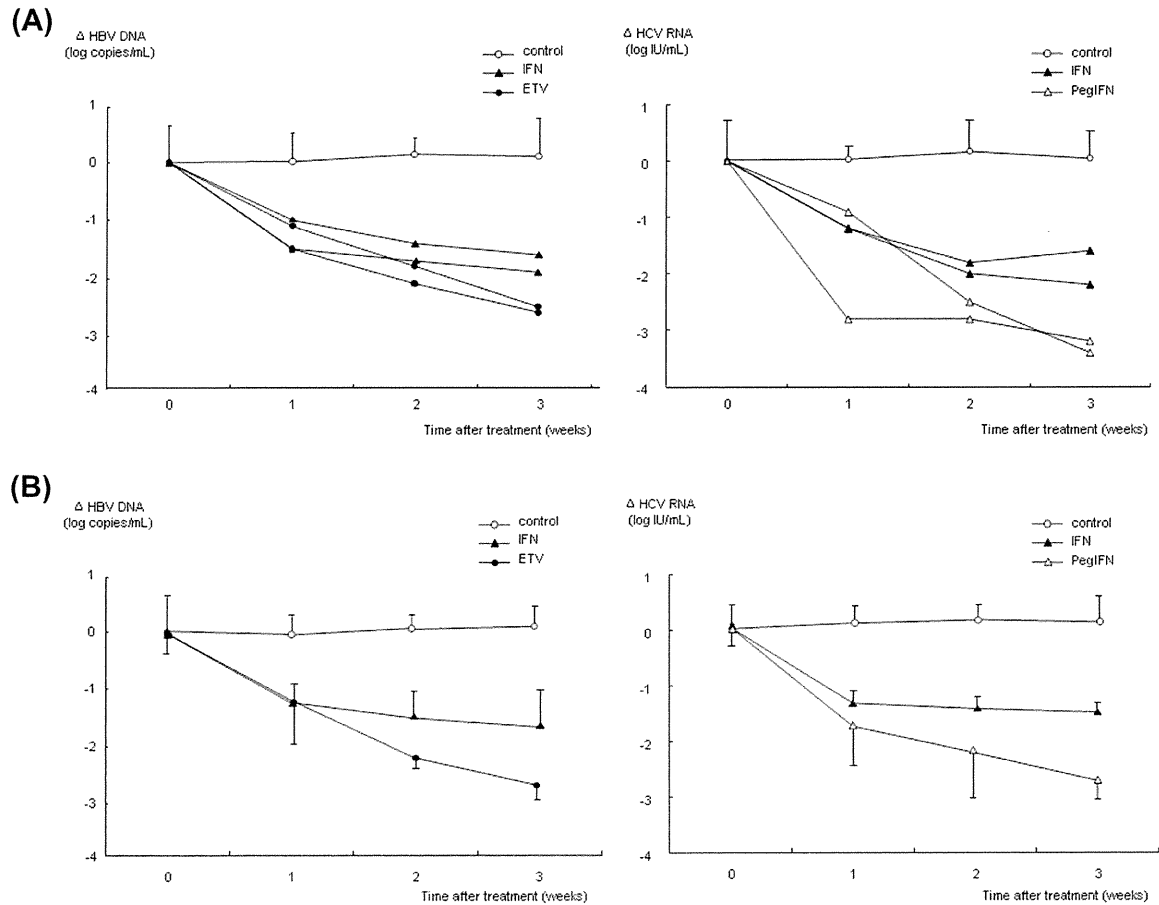


Fig. 3. Reduction of serum viral titers in mice treated with anti-viral agents. (A) HBV- (left panel) or HCV-infected (right panel) TK-NOG mice were treated with entecavir, interferon (IFN)-alpha or PegIFN-alpha-2a. Control: HBV- and HCV-infected mice without antiviral treatment. (B) HBV- (left panel) or HCV-infected (right panel) uPA-SCID mice were treated with entecavir, IFN-alpha or PegIFN-alpha-2a. Data are shown using the mean \pm SD ($n = 4$).

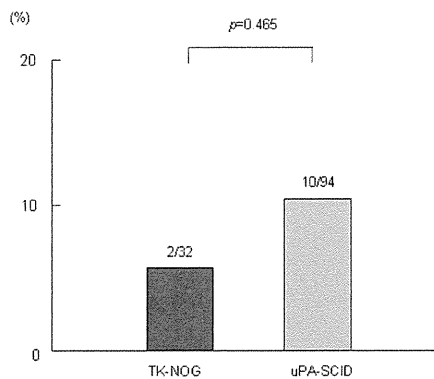


Fig. 4. Frequency of unexpected death within 8 weeks in mice. The numbers of sudden deaths occurring within 8 weeks of viral infection in TK-NOG mice and uPA-SCID mice are shown as bars.

PegIFN-alpha using HBV- and HCV-infected TK-NOG mice and compared them with uPA-SCID mice (Fig. 3). The results showed that both mouse models are equally useful for evaluation of anti-viral drugs.

Human hepatocyte chimeric uPA-SCID mice are weak and prone to unexpected death [20], and this limitation appears to

apply to TK-NOG mice as well. Incidence of unexpected death in the early stages of viral infection was not significantly different between TK-NOG mice and uPA-SCID mice (Fig. 4). The cause of these unexpected deaths is unknown. Further study is necessary to develop a more robust and easy to manipulate animal model.

In summary, we established a hepatitis virus infection mouse model using the human hepatocyte transplanted TK-NOG mouse. This model is useful for the study of hepatitis virology and evaluation of antiviral agents.

Financial support

This work was supported by Grants-in-Aid for scientific research and development from the Ministry of Health, Labor and Welfare and Ministry of Education Culture Sports Science and Technology, Government of Japan. The funders had no role in study design, data collection and analysis, decision to publish, or preparation of the manuscript. No additional external funding was received for this study.

Acknowledgments

The authors thank Rie Akiyama, and Yoko Matsumoto for their expert technical help. This study was supported in part by a Grant-in-Aid for Scientific Research from the Japanese Ministry of Labor, Health and Welfare.